



Fermilab

Accelerator Physics Center

Beam-Material Interactions Part 1

Nikolai Mokhov

Joint International Accelerator School on
"Beam Loss and Accelerator Protection"

Newport Beach, CA, USA

November 7, 2014

Outline

- Introduction
- Interactions of Fast Particles with Matter
- Materials Under Irradiation
- Simulation Tools
- Strong and Electromagnetic Interactions
- DPA and Gas Production Modeling
- Geometry, Beamline Builders and Tallies
- Beamlines, Target Stations, Absorbers
- Protecting SC Magnets and Collider Detectors

Introduction (1)

The next generation of medium- and high-energy accelerators for MegaWatt proton, electron and heavy-ion beams moves us into a completely new domain of extreme energy deposition density up to 0.1 MJ/g and power density up to 1 TW/g in beam interactions with matter.

The consequences of controlled and uncontrolled impacts of such high-intensity beams on components of accelerators, beamlines, target stations, beam collimators and absorbers, detectors, shielding, and environment can range from minor to catastrophic. Challenges also arise from increasing complexity of accelerators and experimental setups, as well as from design, engineering and performance constraints.

Introduction (2)

All these put unprecedented requirements on the accuracy of particle production predictions, the capability and reliability of the codes used in planning new accelerator facilities and experiments, the design of machine, target and collimation systems, new materials and technologies, detectors, and radiation shielding and minimization of their impact on environment.

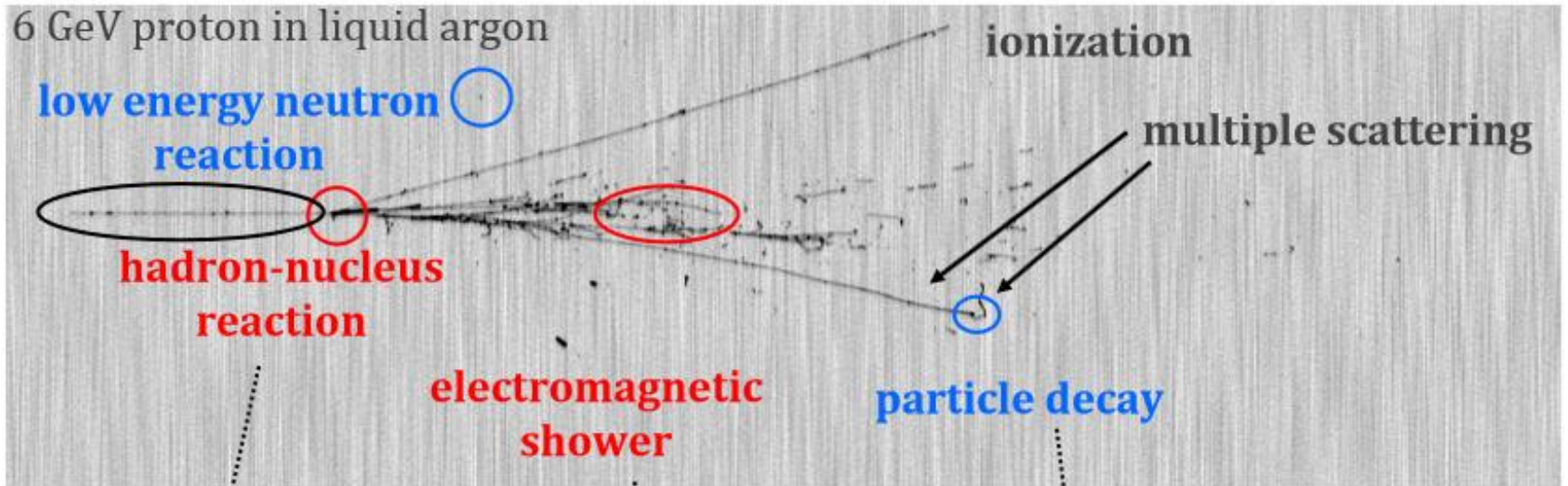
Particle transport simulation tools and the physics models and calculations required in developing relevant codes are all driven by application. The most demanding applications are the high-power accelerators (e.g., spallation neutron sources, heavy-ion machines, and neutrino factories), Accelerator Driven Systems (ADS), high-energy colliders, and medical facilities.

Interactions of Fast Particles with Matter (1)

Electromagnetic interactions, decays of unstable particles and strong inelastic and elastic nuclear interactions all affect the passage of high-energy particles through matter. At high energies the characteristic feature of the phenomenon is creation of hadronic cascades and electromagnetic showers (EMS) in matter due to multi-particle production in electromagnetic and strong nuclear interactions.

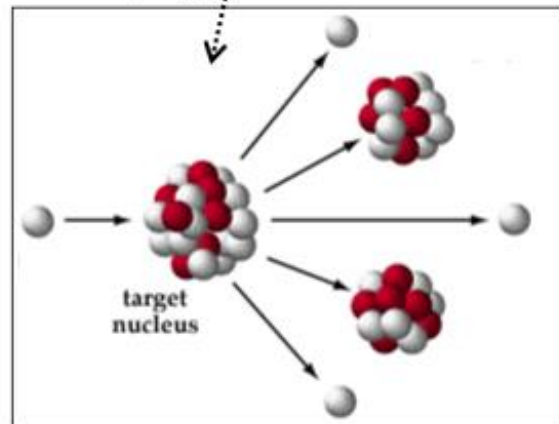
Because of consecutive multiplication, the interaction avalanche rapidly accrues, passes the maximum and then dies as a result of energy dissipation between the cascade particles and due to ionization energy loss. Energetic particles are concentrated around the projectile axis forming the shower core. Neutral particles (mainly neutrons) and photons dominate with a cascade development when energy drops below a few hundred MeV.

Microscopic View

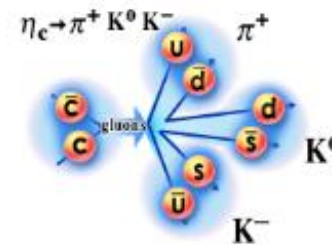
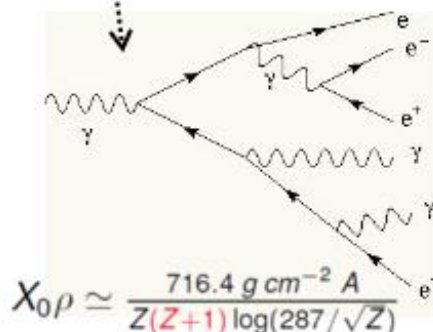


$$\lambda\rho = \frac{A}{\sigma_R N_A}$$

$$\sigma_R \simeq \pi r_0^2 A^{2/3}$$



interplay of many physical processes described by different theories/models



Interactions of Fast Particles with Matter (2)

The length scale in hadronic cascades is a nuclear interaction length λ_I (16.8 cm in iron) while in EMS it is a radiation length X_0 (1.76 cm in iron). The hadronic cascade longitudinal dimension is $(5-10) \lambda_I$, while in EMS it is $(10-30) X_0$. It grows logarithmically with primary energy in both cases. Transversely, the effective radius of hadronic cascade is about λ_I , while for EMS it is about $2r_M$, where r_M is a Moliere radius $R_M = 0.0265 X_0 (Z+1.2)$. Low-energy neutrons coupled to photons propagate much larger distance in matter around cascade core, both longitudinally and transversely, until they dissipate their energy in a region of a fraction of an electronvolt.

Muons - created predominantly in pion and kaon decays during the cascade development – can travel hundreds and thousands of meters in matter along the cascade axis. Neutrinos – usual muon partners in such decays – propagate even farther, hundreds and thousands of kilometers, until they exit the Earth's surface.

Materials Under Irradiation

Depending on material, level of energy deposition density and its time structure, one can face a variety of effects in materials under irradiation.

Component damage (lifetime):

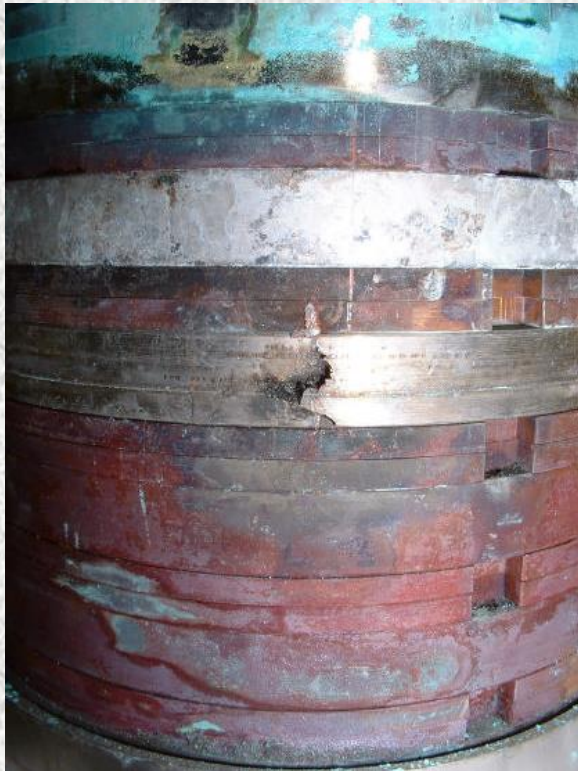
- Thermal shocks and quasi-instantaneous damage
- Insulation property deterioration due to dose buildup
- Radiation damage to inorganic materials due to atomic displacements and helium production.

Operational (performance):

- Superconducting magnet quench
- Single-event effects in electronics
- Detector performance deterioration
- Radioactivation, prompt dose and impact on environment

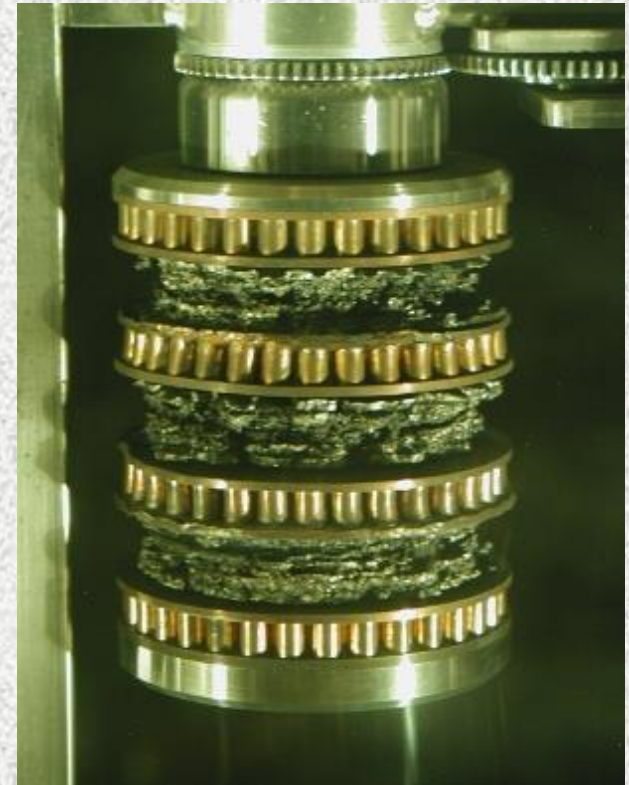
Example: Thermal Shock

Short pulses with energy deposition density EDD in the range from 200 J/g (W), 600 J/g (Cu), ~1 kJ/g (Ni, Inconel) to ~15 kJ/g: thermal shocks resulting in fast ablation and slower structural changes.



FNAL pbar production target under 120-GeV p-beam ($3e12$ ppp, $\sigma \sim 0.2$ mm)

MARS simulations explained target damage, reduction of pbar yield and justified better target materials

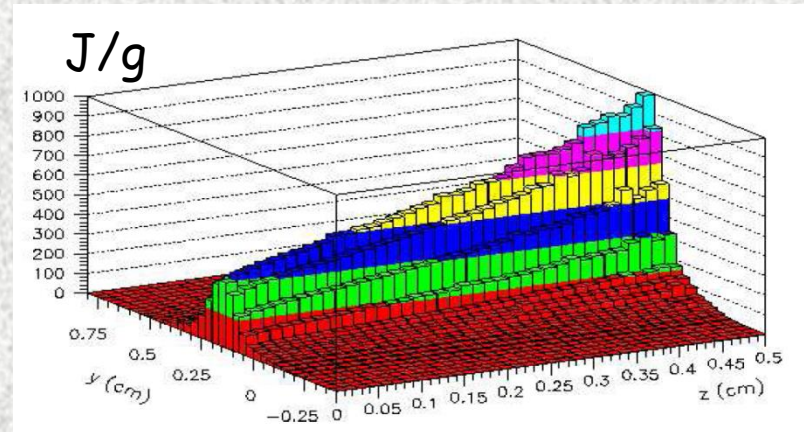
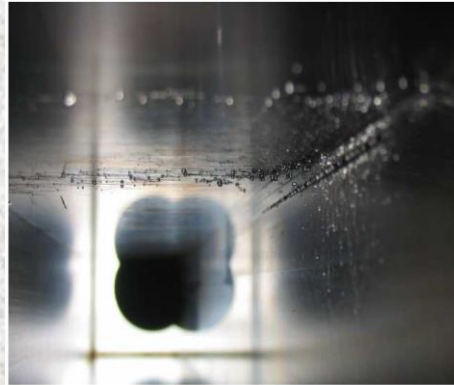


Example: Tevatron Collimator Damage in 2003

Hole in 5-mm W



25-cm groove in SS



Detailed modeling of dynamics of beam loss (STRUCT), energy deposition (MARS15) and time evolution over 1.6 ms of the tungsten collimator ablation, fully explained what happened.

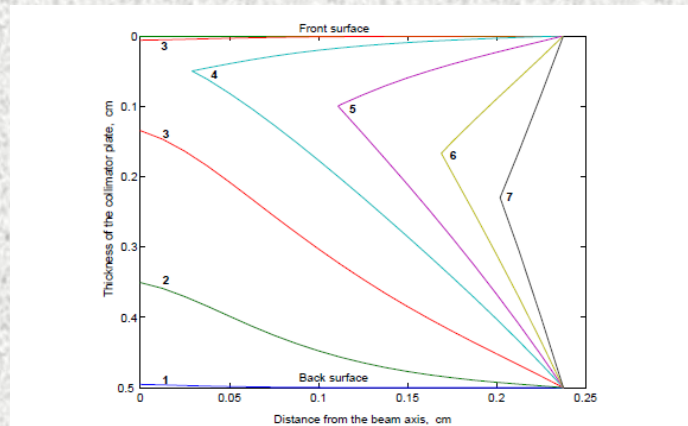
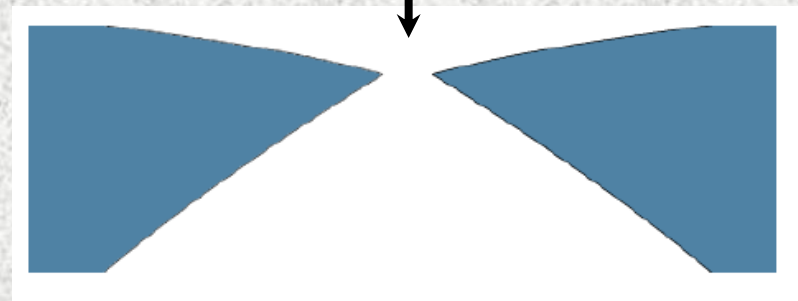


Figure 7: Evolution of the front and back surfaces of the collimator plate at $t = 0.4_{[1]} - 1.6_{[7]} ms$ with $\Delta t = 0.2 ms$.

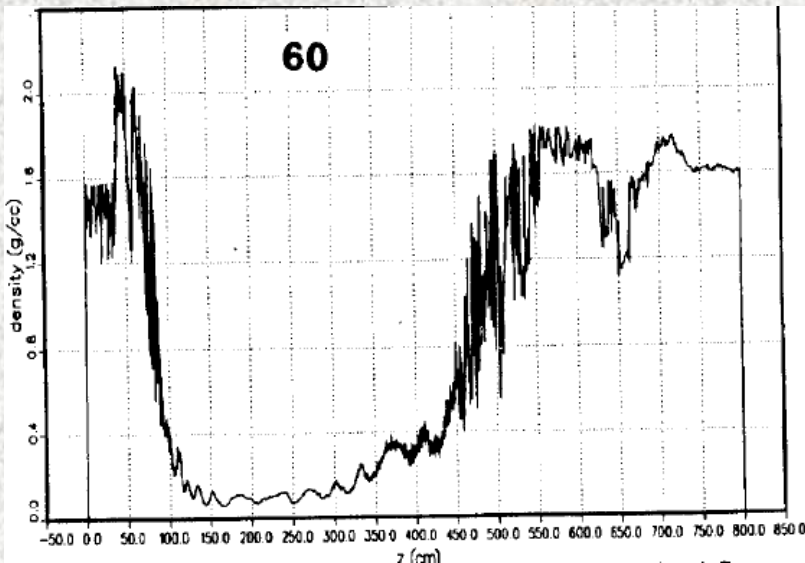
980-GeV p-beam



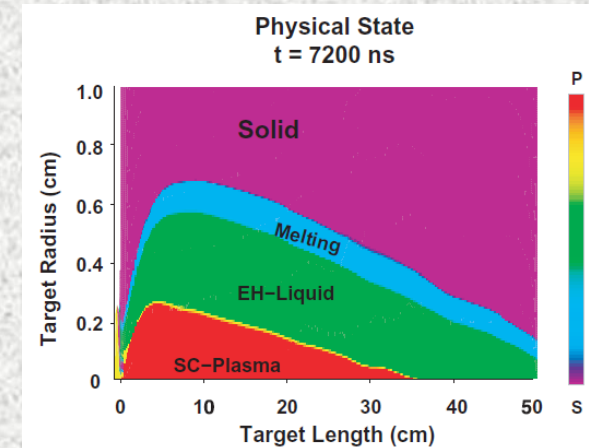
Hydrodynamics in Solid Materials

Pulses with EDD >15 kJ/g: hydrodynamic regime.

First done for the 300- μ s, 400-MJ, 20-TeV proton beams for the SSC graphite beam dump, steel collimators and tunnel-surrounding Austin Chalk by SSC-LANL Collaboration (D. Wilson, ..., N. Mokhov, PAC93, p. 3090). Combining MARS ED calculations at each time step for a fresh material state and MESA/SPHINX hydrodynamics codes.



The hole was drilled at the 7 cm/ μ s penetration rate. Shown is axial density of graphite beam dump in 60 μ s after the spill start.



Later, studies by N. Tahir et al with FLUKA+BIG2 codes for SPS & LHC

These days we use MARS+FRONTIER.

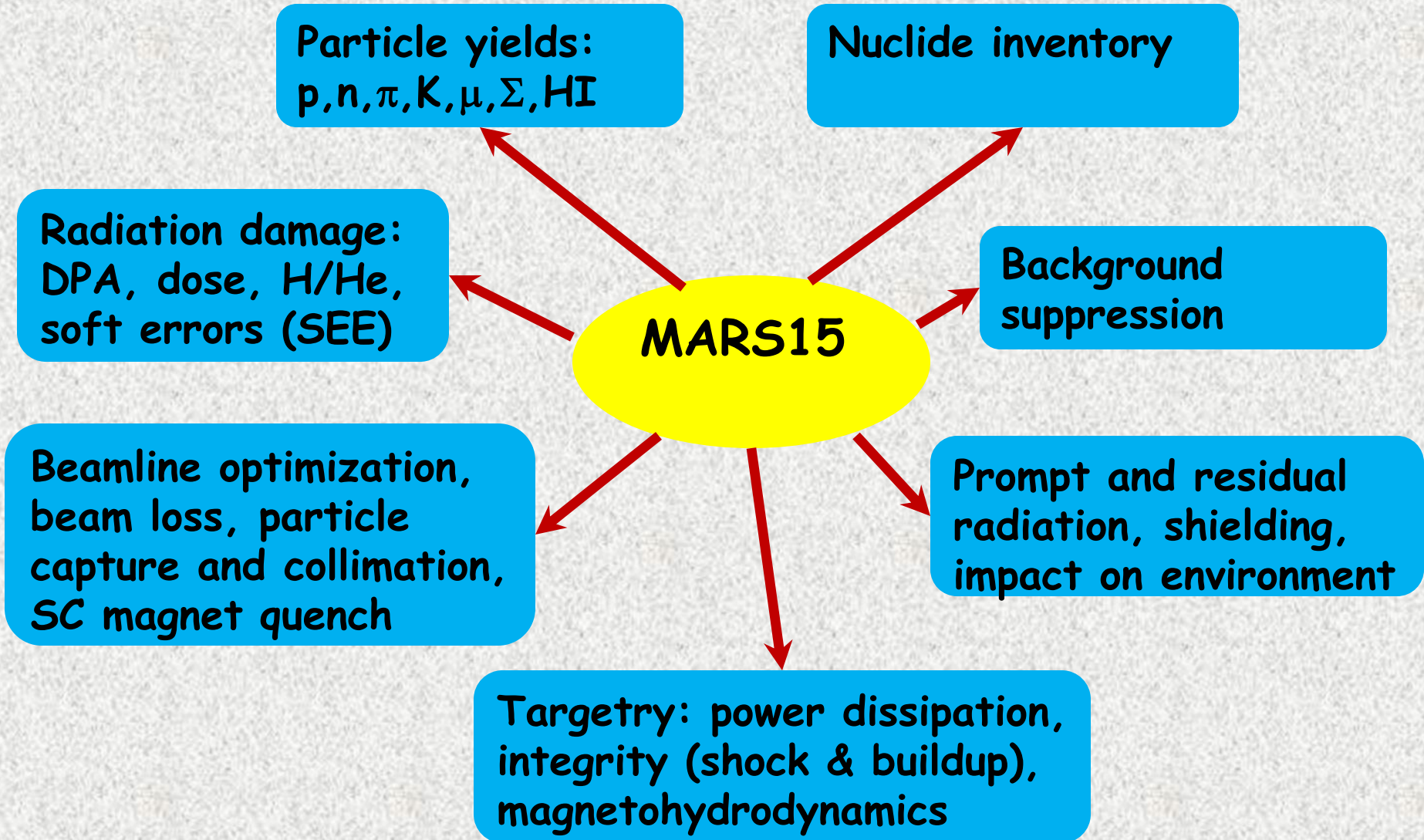
See more in Bertarelli's lecture tomorrow

Simulation Tools

The challenge is detailed and accurate (to a % level) modeling of all particle interactions with 3-D system components (up to tens of kilometers of the accelerator lattice in some cases) in energy region spanning up to 20 decades as a basis of accelerator, detector and shielding designs and their performance evaluation, for both short-term and long-term effects.

The current versions of five general-purpose, all-particle codes are capable of this: FLUKA, GEANT4, MARS15, MCNP6, and PHITS. These are used extensively worldwide for accelerator applications in concert with such particle tracking codes as SixTrack. A substantial amount of effort (up to several hundreds of man-years) has been put into development of these codes over the last few decades. The user communities for the codes reach several thousands of people worldwide.

Example: MARS15 Code for Intensity Frontier



Simulation Tools (2)

The five codes listed above can handle a very complex geometry, have powerful user-friendly built-in Graphical-User Interfaces (GUI) with magnetic field and tally viewers, and variance reduction capabilities.

Tallies include volume and surface distributions (1D to 3D) of particle flux, energy, reaction rate, energy deposition, residual nuclide inventory, prompt and residual dose equivalent, displacement-per-atom (DPA) for radiation damage, event logs, intermediate source terms, etc.

All the aspects of beam interactions with accelerator system components are addressed in sophisticated Monte-Carlo simulations benchmarked - wherever possible - with dedicated beam tests.

Particle Production in Nuclear Interactions

- The origin of the majority of beam-induced deleterious effects in accelerator, detector, beamlines, targets, collimators, absorbers and environment.
- The key for fixed target and collider experiment planning.
- Models are OK at $E_p < 1-3$ GeV and $E_p > 8-10$ GeV.
- At intermediate energies, most interesting for the Intensity Frontier: some theoretical difficulties; experimental data contradict each other; the main problem with low-energy pion production that is crucial for many experiments.

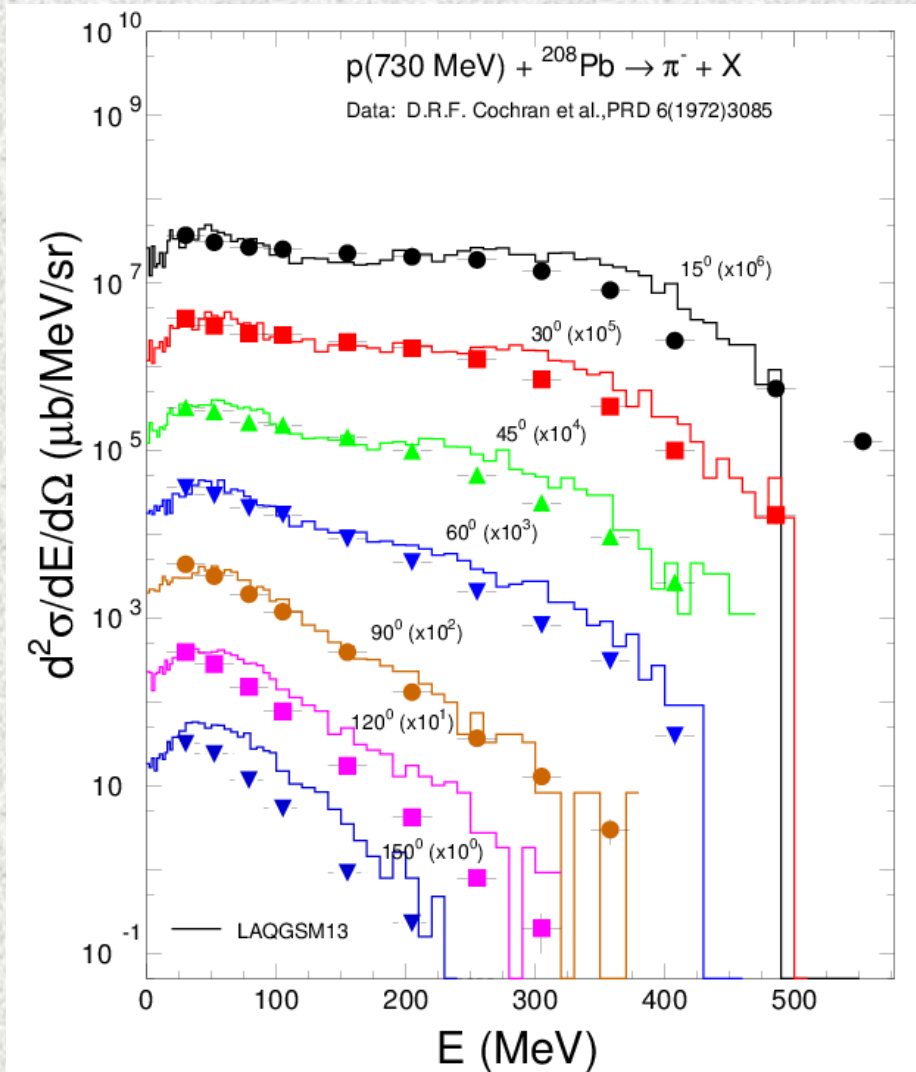
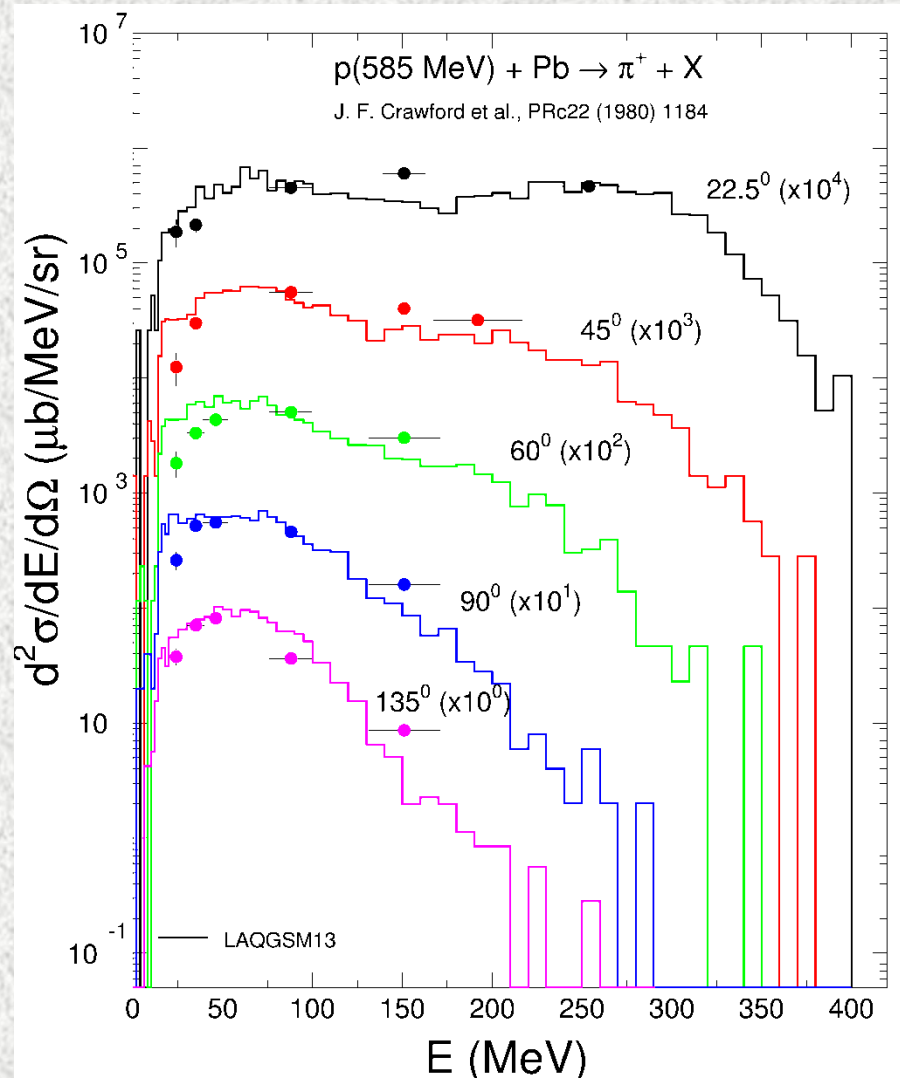
Example: MARS15 Exclusive Event Generator

The Los Alamos Quark-Gluon String Model code, [LAQGSM \(2013\)](#), is used in MARS15 for photon, particle and heavy-ion projectiles at a few MeV/A to 1 TeV/A. This provides a power of full theoretically consistent modeling of exclusive and inclusive distributions of secondary particles, spallation, fission, and fragmentation products.

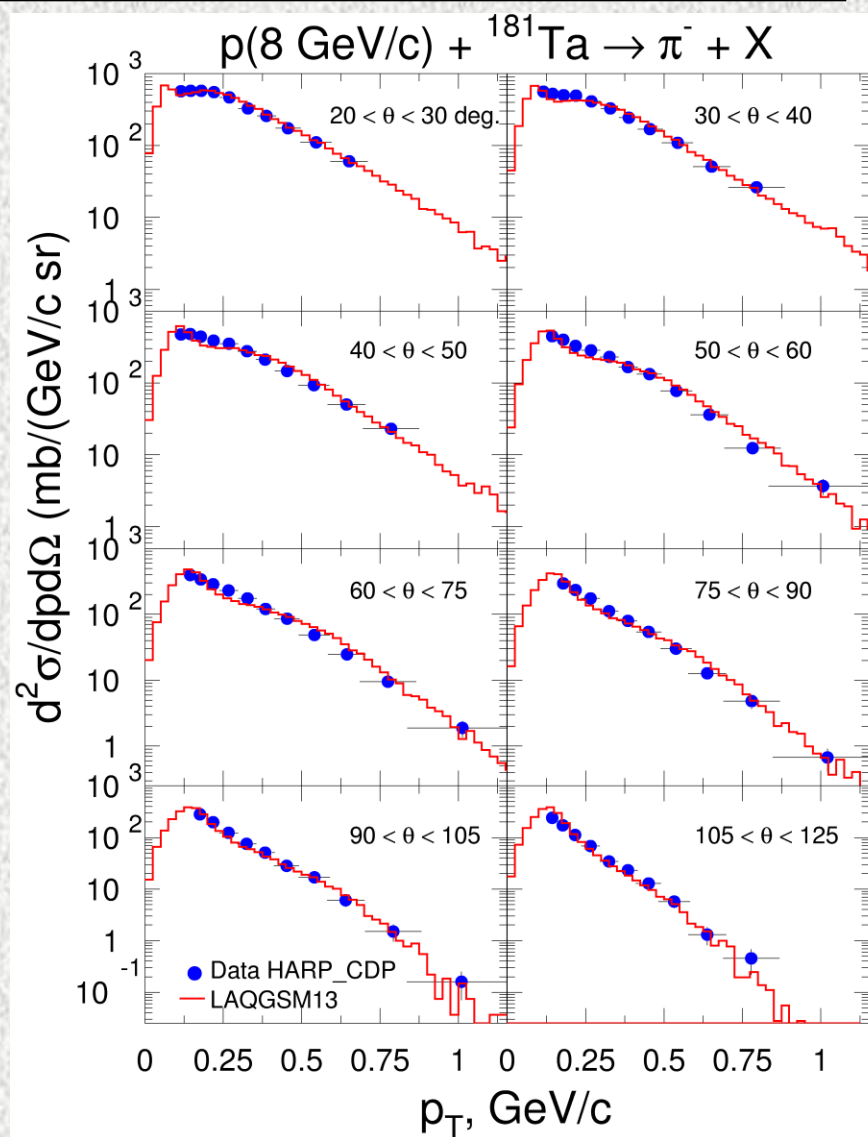
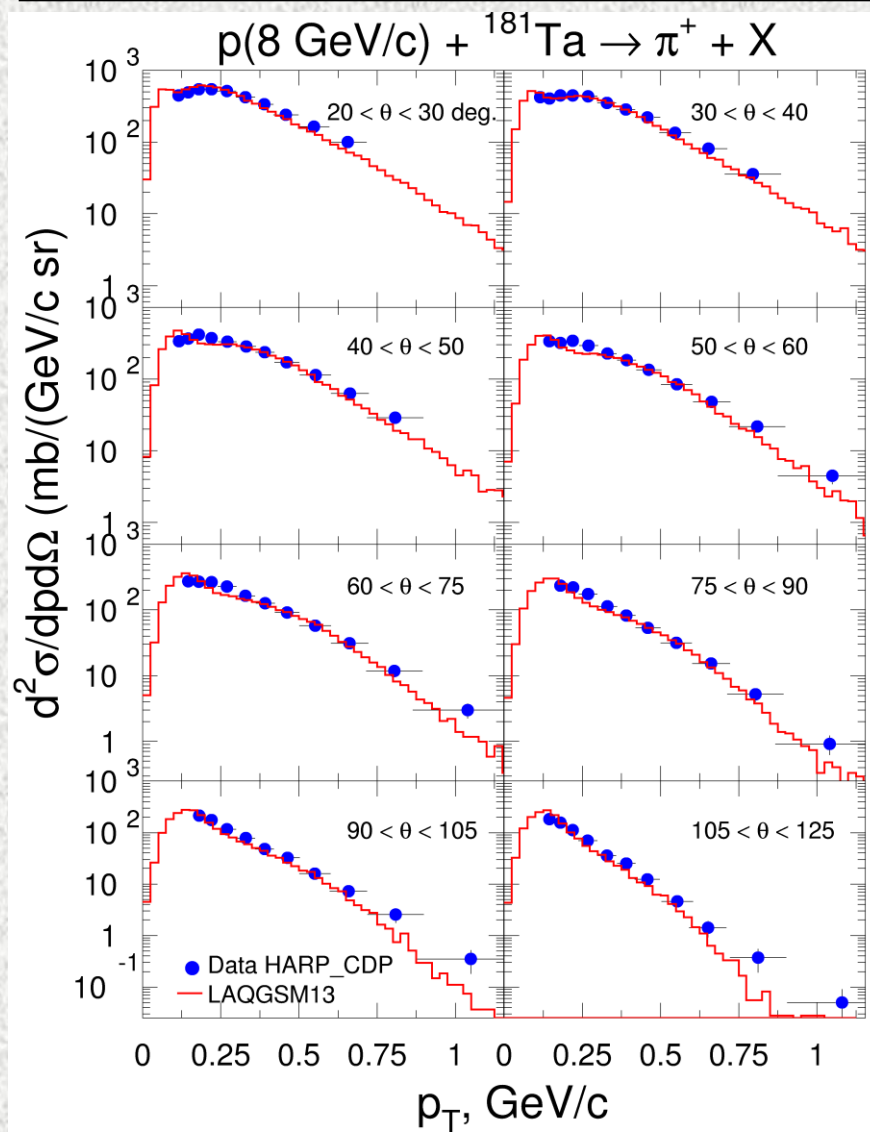
Recent improvements:

- New and better approximations for elementary total, elastic, and inelastic cross sections for NN and π N interactions
- Several channels have been implemented for an explicit description:
 $N+N \rightarrow N+N+m\pi$, $\pi+N \rightarrow N+m\pi$ ($m < 5$), $B+B \rightarrow B+Y+K$, $\pi+B \rightarrow Y+K$, $K\bar{K}+B \rightarrow Y+\pi$, and $K+K\bar{K}$, $N+N\bar{K}$ pair production
- Arbitrary light nuclear projectile (e.g., d) and nuclear target (e.g., He)
- Phenomenological parameterization of cross section of pion absorption on NN pair in nuclear medium was constructed based on $\pi+d$ cross section $\sigma(A,T) = P(A) \times \sigma(\pi+d)$ with $P(A) = \alpha A^\beta$. Absorption probability is proportional to nucleon density squared $\rho^2(r)$.
- Improved description of pion absorption in nuclei in $\Delta+N \rightarrow NN$.
- New channel for pion production near threshold in $N+N \rightarrow \pi+d$.

LAQGSM Performance at 585 and 730 MeV

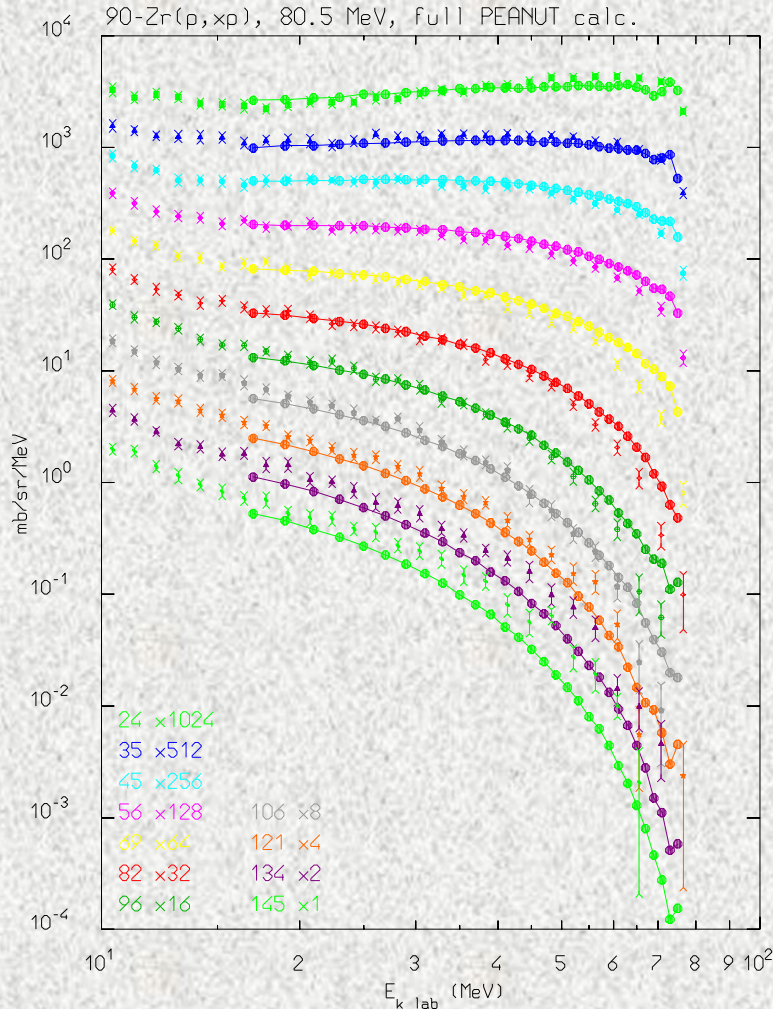


LAQGSM2013 vs HARP-CDP DATA at 8 GeV/c



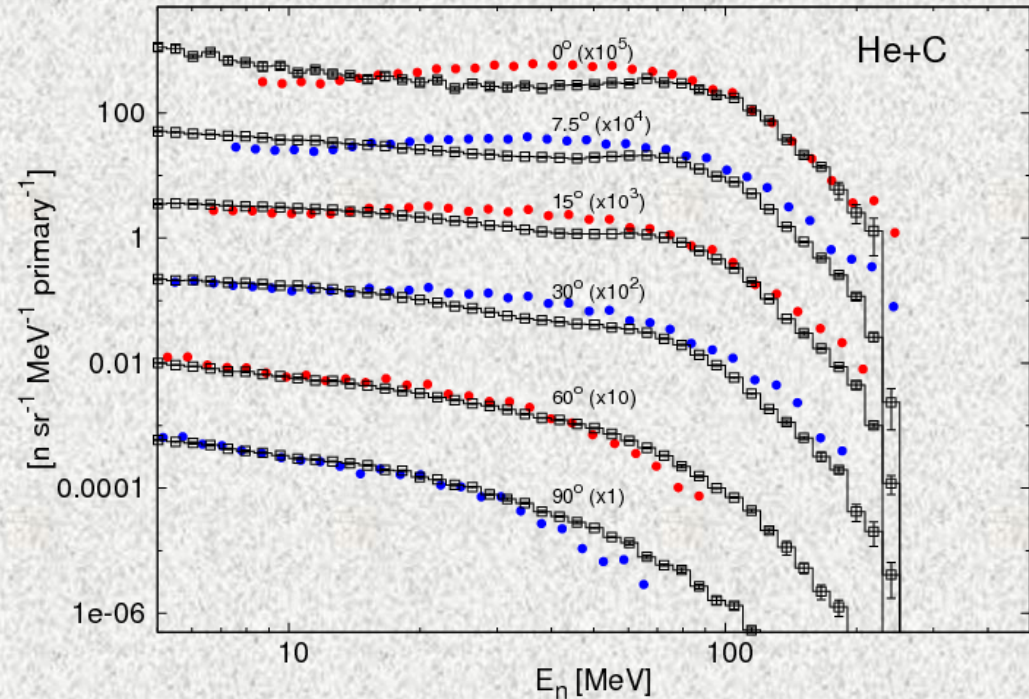
FLUKA: Nucleon Production at 80 and 400 MeV

80 MeV p + ^{90}Zr \rightarrow p + X



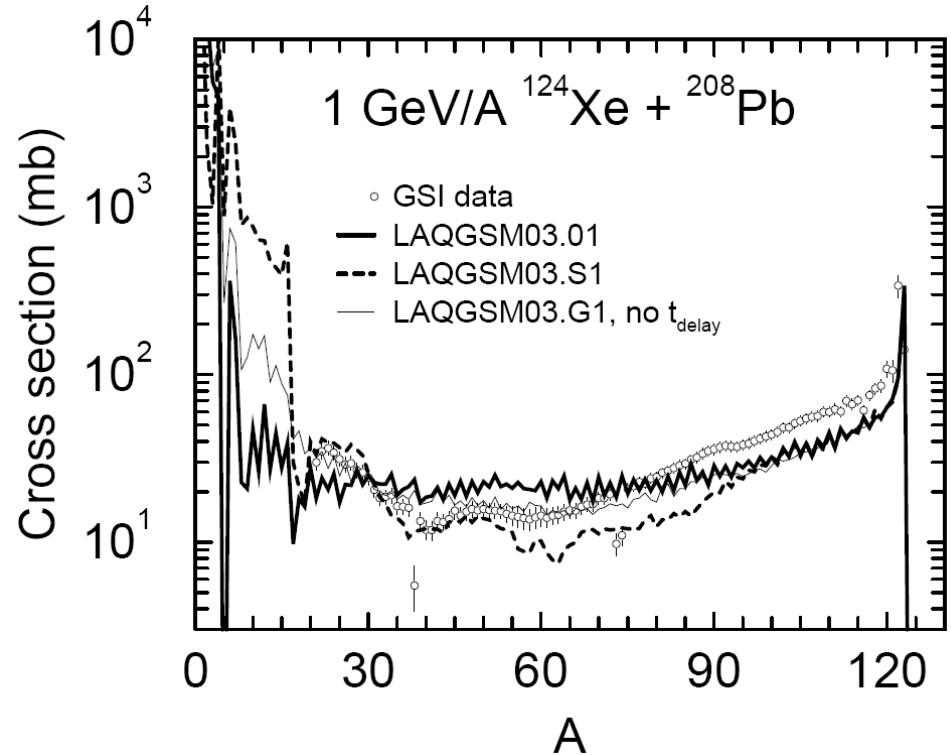
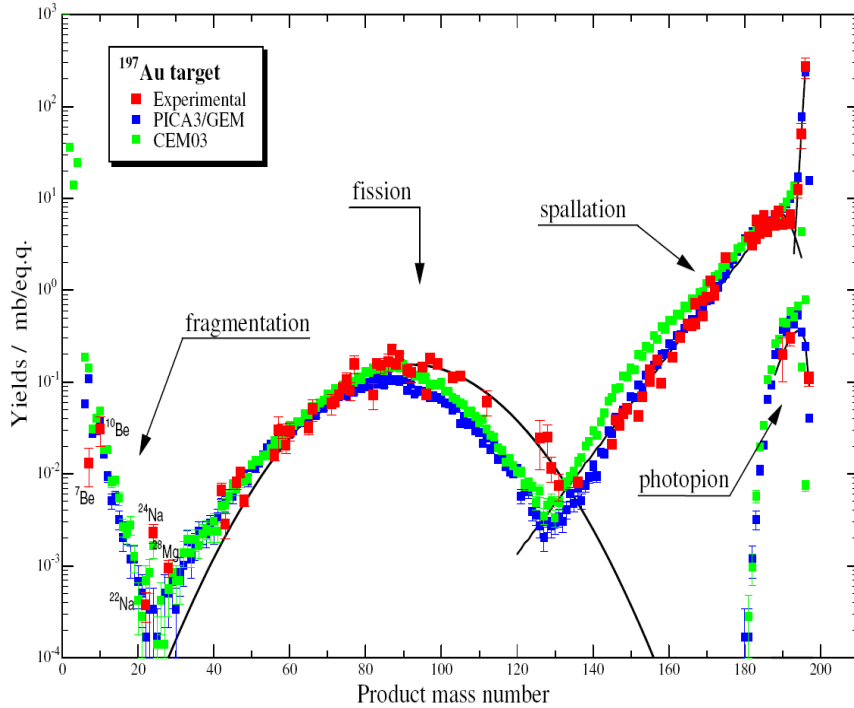
Thick target

Neutrons from 400 MeV α on carbon



Nuclide Production in CEM & LAQGSM

Bremsstrahlung ($E_{\text{max}}=1 \text{ GeV}$) on gold

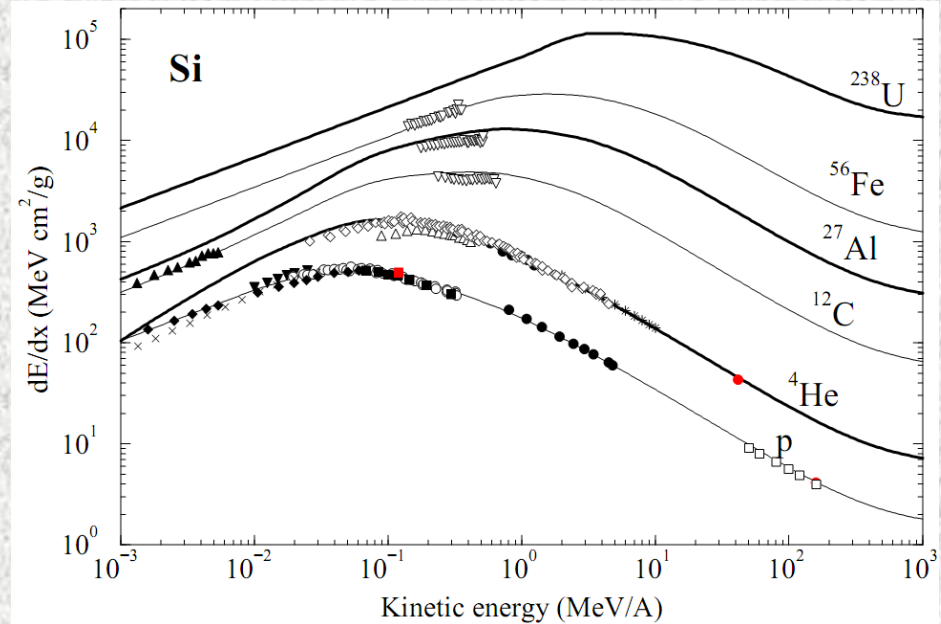


Mean Stopping Power

$$-\frac{1}{\rho} \frac{dE}{dx} = 4\pi N_A r_e^2 m_e c^2 z^2 \frac{Z}{A} \frac{1}{\beta^2} L(\beta)$$

$$L(\beta) = L_0(\beta) + \sum_i \Delta L_i$$

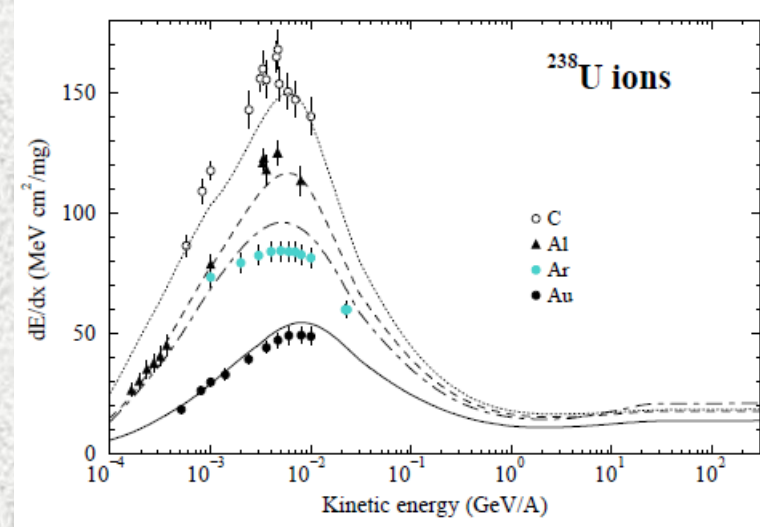
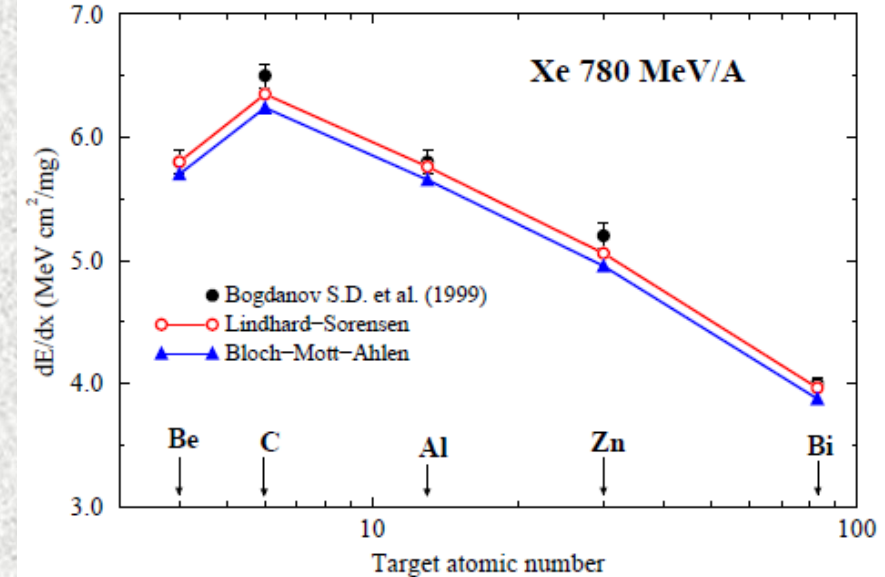
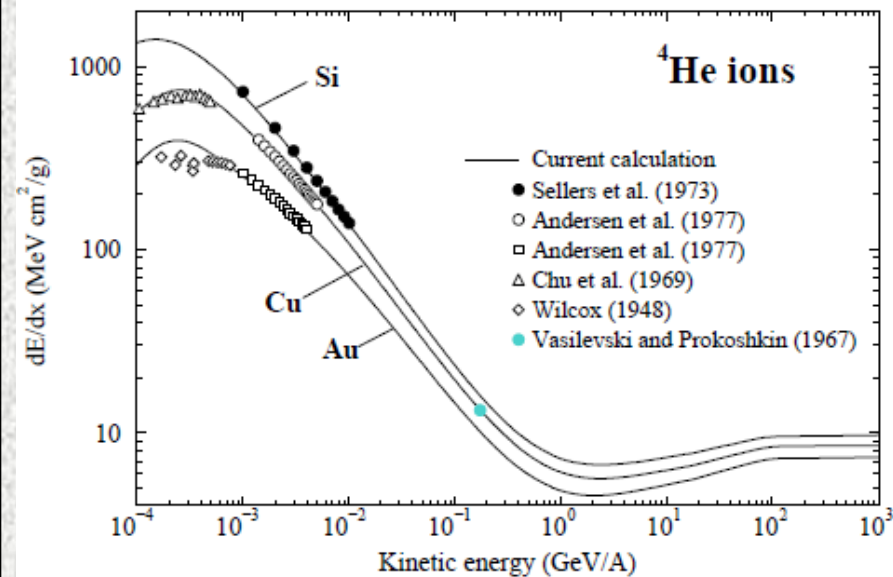
$$L_0(\beta) = \ln\left(\frac{2m_e c^2 \beta^2 \gamma^2}{I}\right) - \beta^2 - \frac{\delta}{2}$$



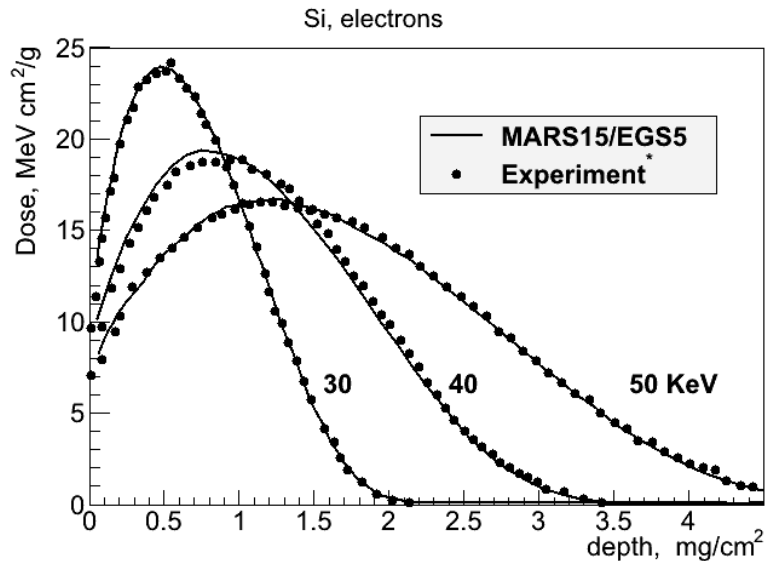
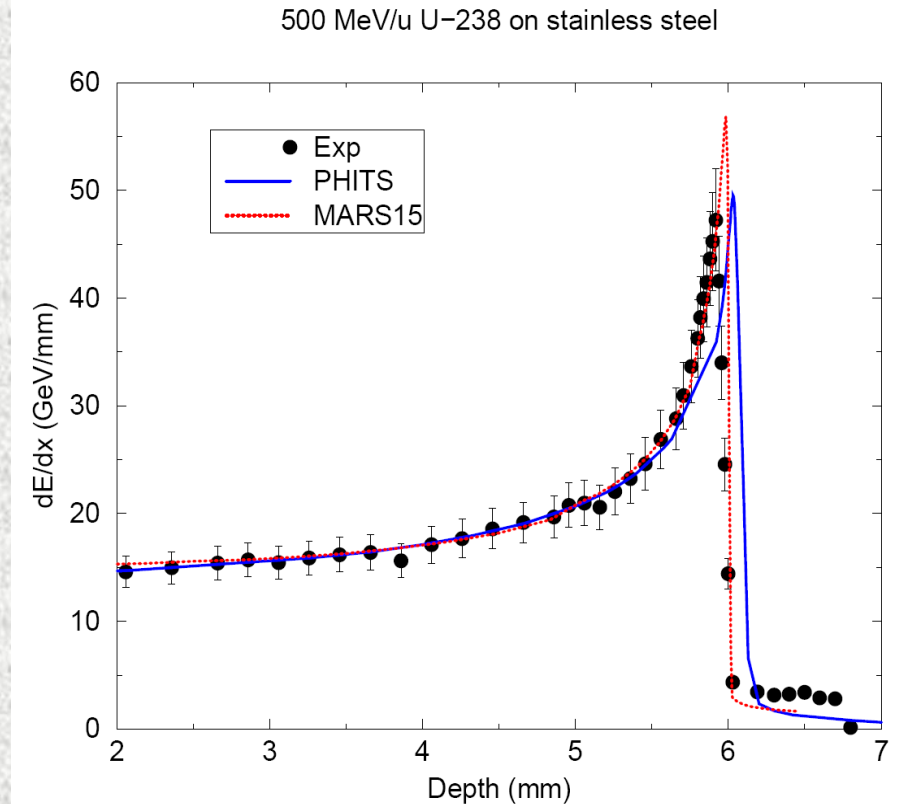
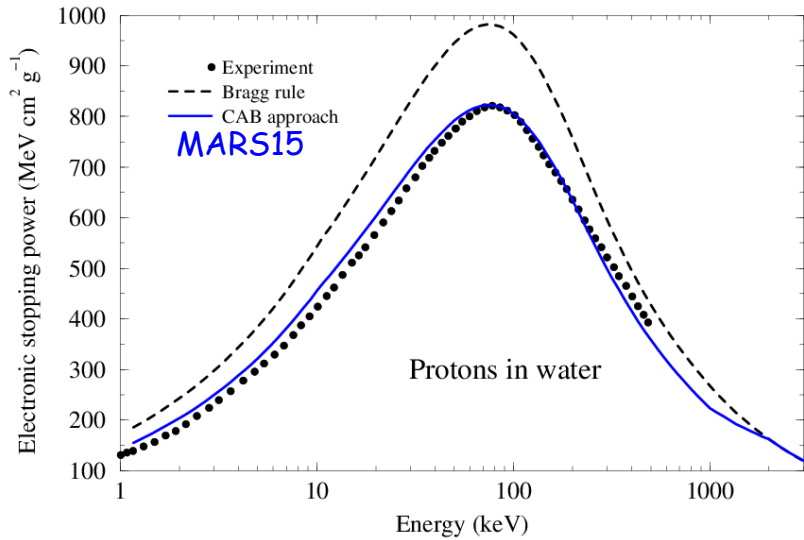
- ΔL_i : (i) **Lindhard-Sørensen** correction (exact solution to the Dirac equation; terms higher than z^2);
 (ii) **Barkas** correction (target polarization effects due to low-energy distant collisions);
 (iii) **shell** correction;

Projectile **effective charge** comes separately as a multiplicative factor that takes into account electron capture at low projectile energies (e.g., $z_{\text{eff}} \sim 20$ for 1-MeV/A ^{238}U in Al, instead of bare charge of 92).

Heavy-Ion Energy Loss in MARS15

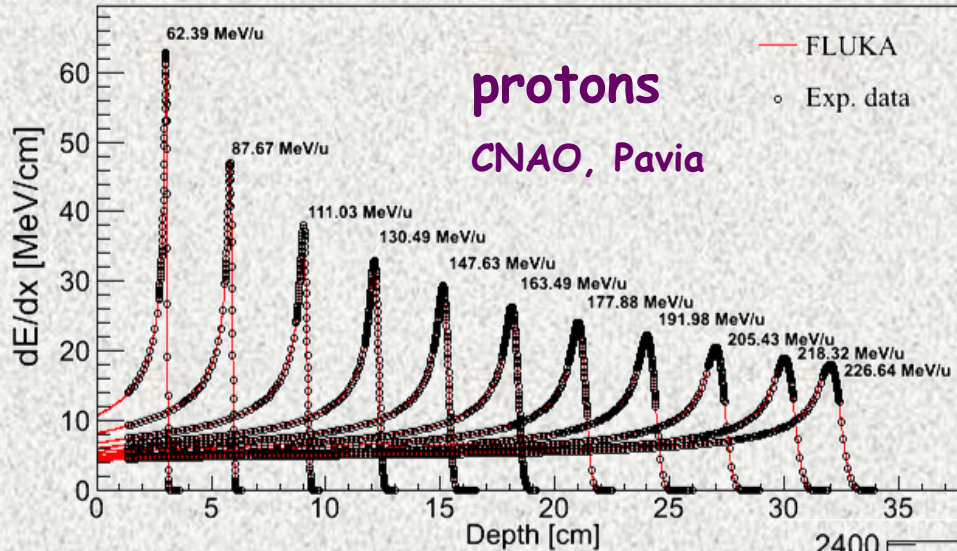


Energy Deposition Modeling: Highly Accurate



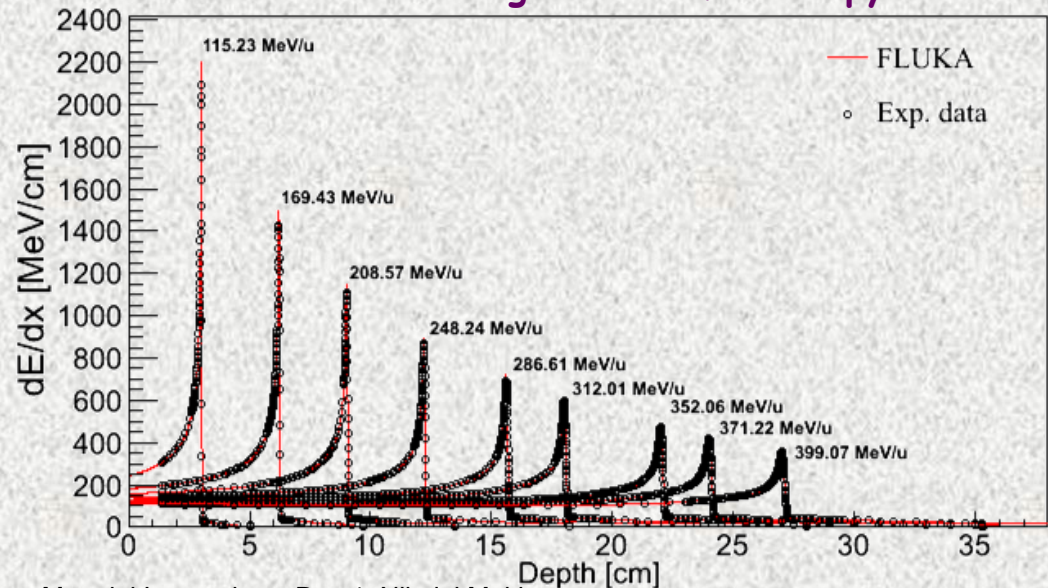
In majority of real-life complex applications, FLUKA and MARS15 energy deposition results coincide within a few % and agree with data.

FLUKA: Depth-Dose for p & C in Water



^{12}C ions in water

Heidelberg Ion-Beam Therapy Center



DPA Model

$$\sigma_d(E) = \int_{T_d}^{T_{\max}} \frac{d\sigma(E,T)}{dT} v(T) dT$$

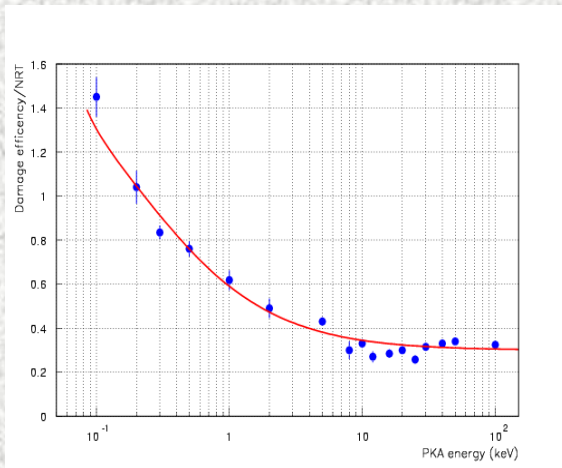
NRT damage function:

$$v(T) = \begin{cases} 0 & (T < T_d) \\ 1 & (T_d \leq T < 2.5T_d) \\ k(T)E_d/2T_d & (2.5T_d \leq T) \end{cases}$$

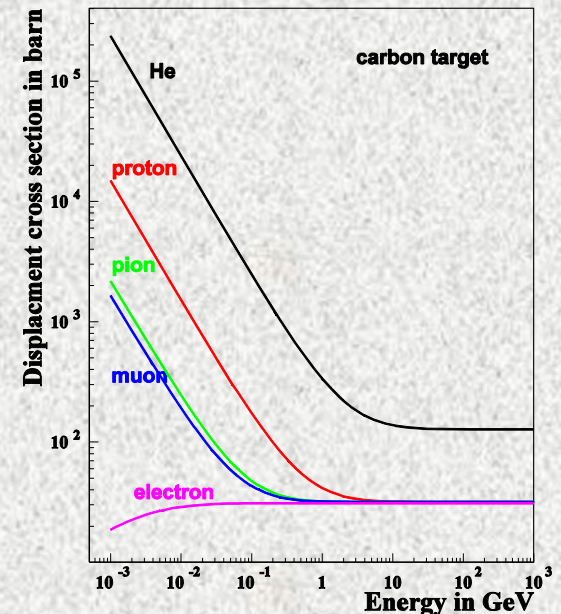
T_d is displacement energy (~ 40 eV)

E_d is damage energy (\sim keV)

Energy-dependent displacement efficiency $k(T)$ by Stoller/Smirnov:



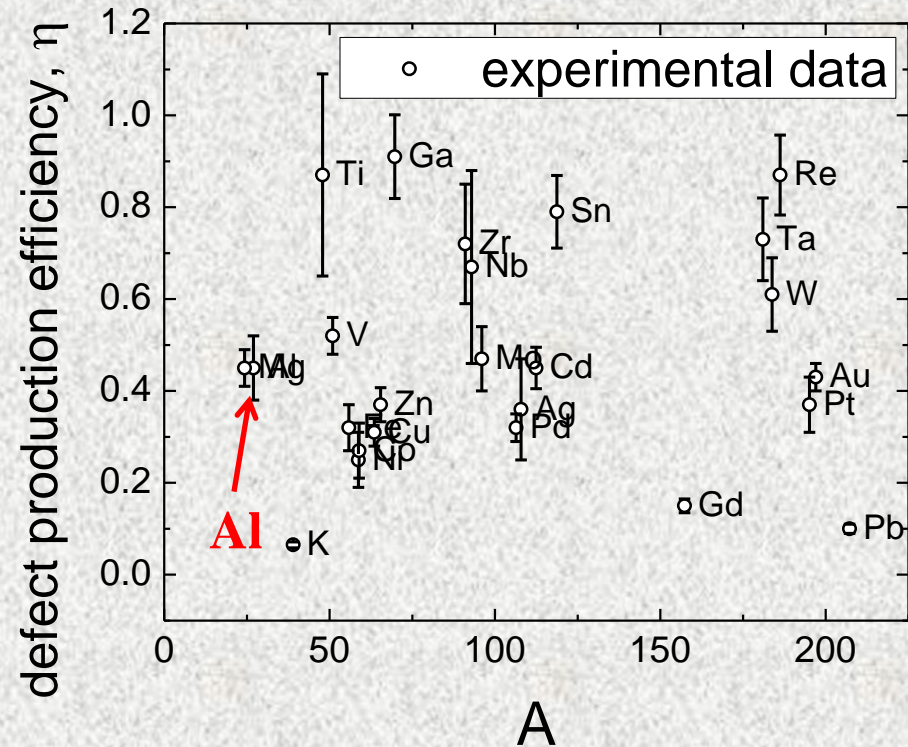
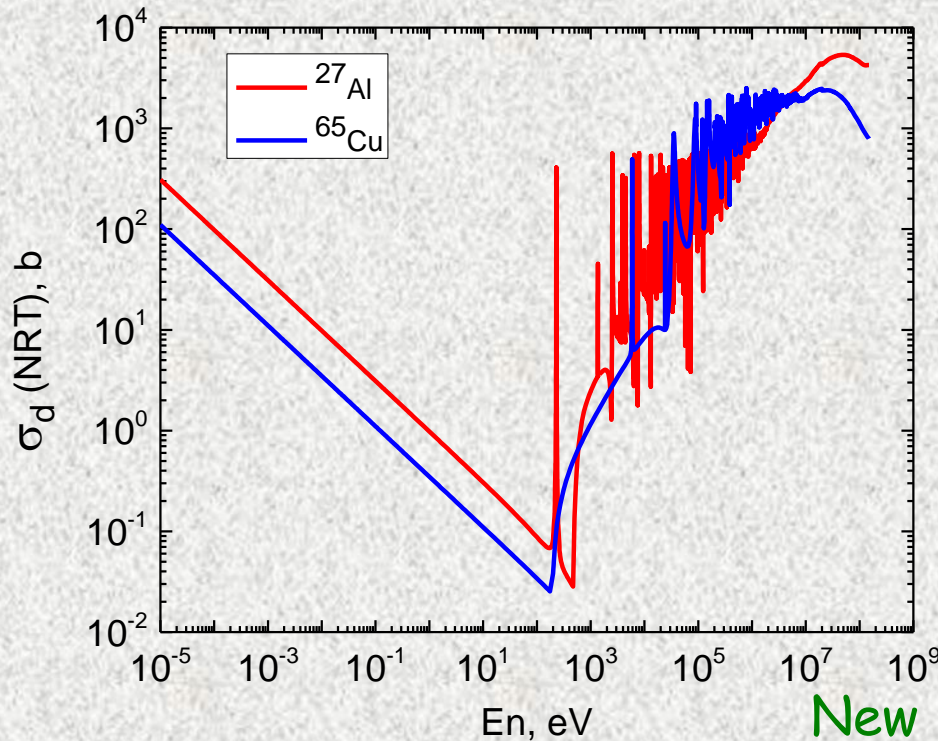
All products of elastic and inelastic nuclear interactions as well as Coulomb elastic scattering (NIEL) of transported charged particles (hadrons, electrons, muons and heavy ions) from 1 keV to 10 TeV contribute to DPA in this model. For electromagnetic elastic (Coulomb) scattering, Rutherford cross section with Mott corrections and nuclear form factors are used.



DPA is the most universal way to characterize the impact of irradiation on inorganic materials

Medium- and Low-E Neutron DPA Model in MARS15 and Optional Correction at Cryo Temperatures

T = 4-6 K

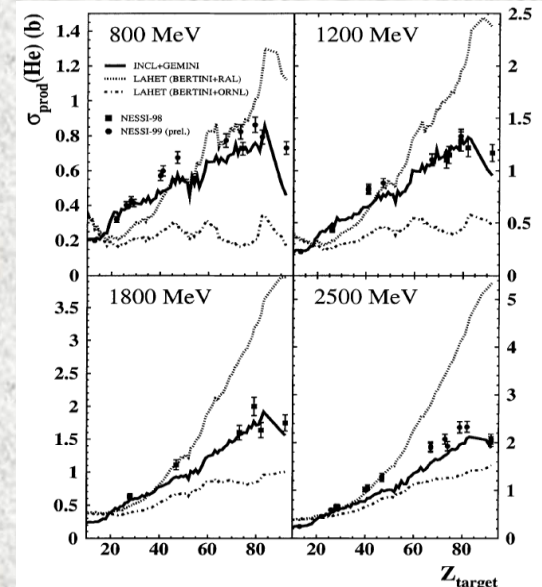
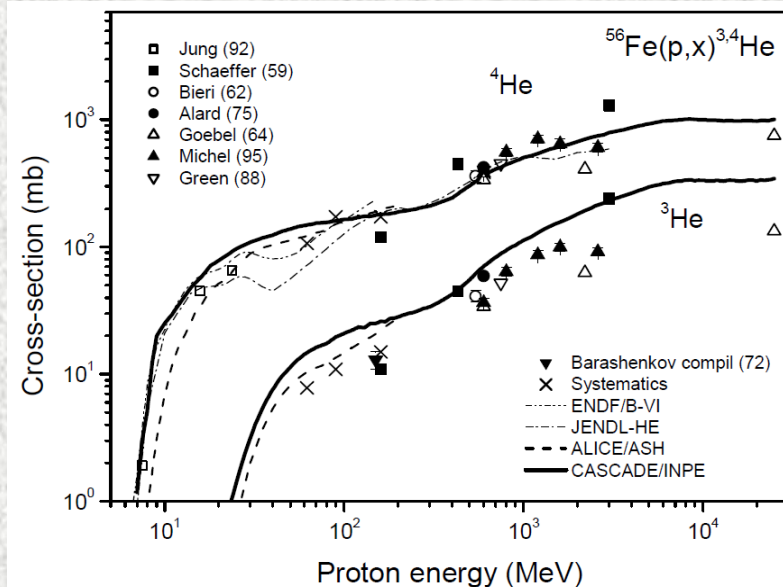


For neutrons from 10^{-5} eV to 150 MeV: NJOY99+ENDF-VII database, for 393 nuclides. At T=4-6K, optional correction for experimental defect production efficiency η (Broeders, Konobeev, 2004), where η is a ratio of a number of single interstitial atom vacancy pairs (Frenkel pairs) produced in a material to the number of defects calculated using NRT model

Hydrogen and Helium Gas Production

At accelerators, radiation damage to structural materials is amplified by increased hydrogen and helium gas production for high-energy beams. In SNS-type beam windows, the ratio of He/atom to DPA is about 500 of that in fission reactors. These gases can lead to grain boundary embrittlement and accelerated swelling.

In modern codes at intermediate energies, uncertainties on production of hydrogen are ~20%. For helium these could be up to 50%.



C. Broeders, A. Konobeyev, FZKA 7197 (2006)

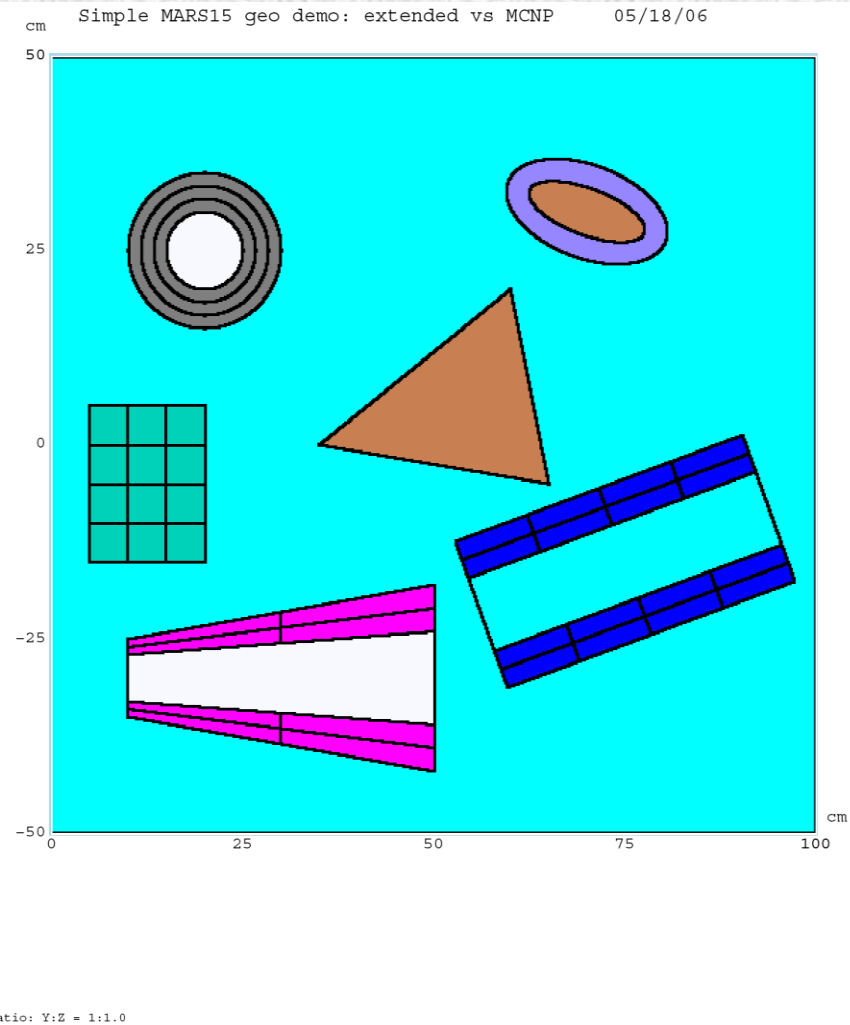
D. Hilscher et al., J.Nucl.Mat, 296(2001)83

SIMPLE GEO EXAMPLE: GEOM.INP

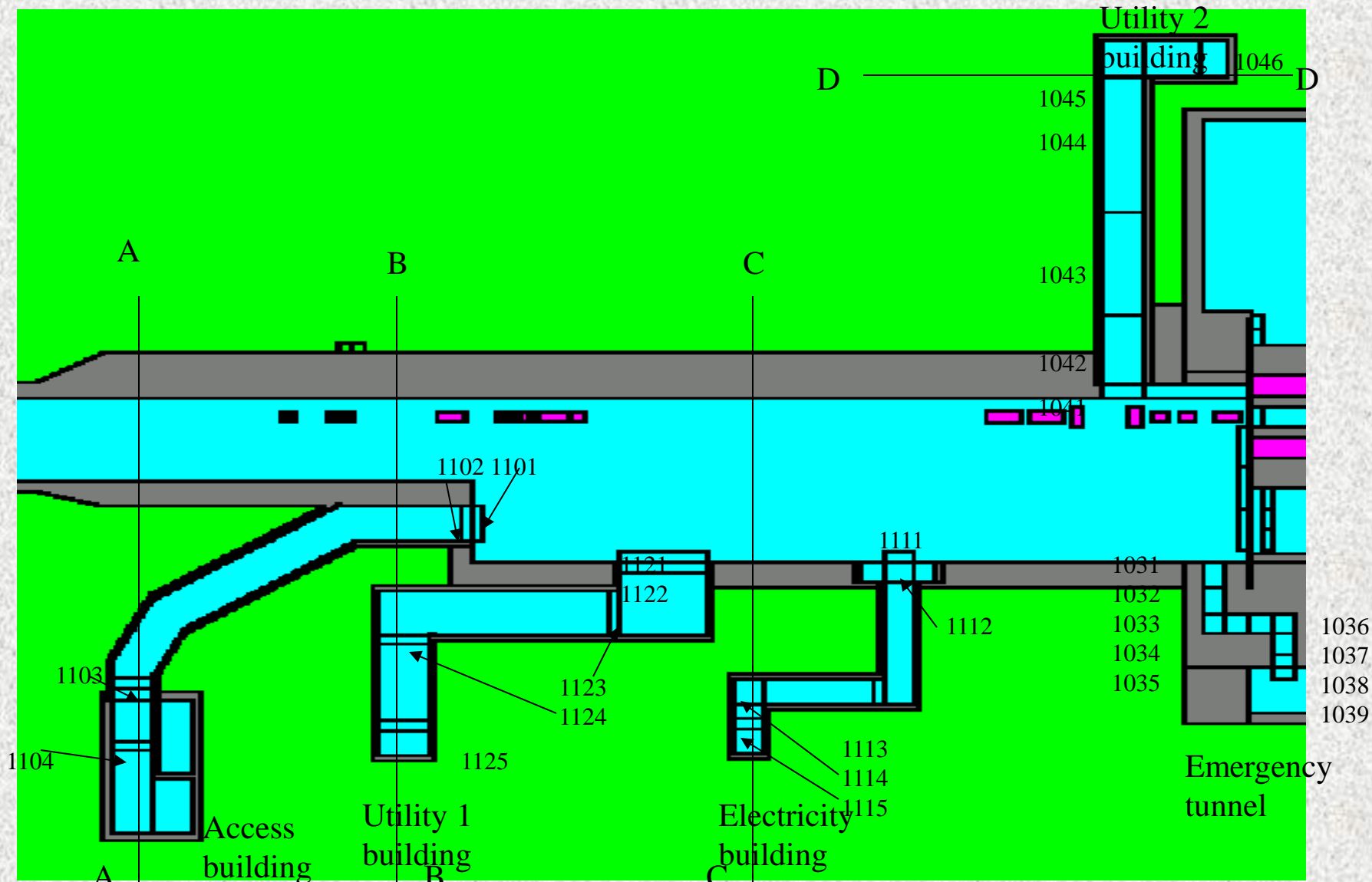
Extended Demo 05/17/06

~~OPT~~ this card is obsolete 2014' version

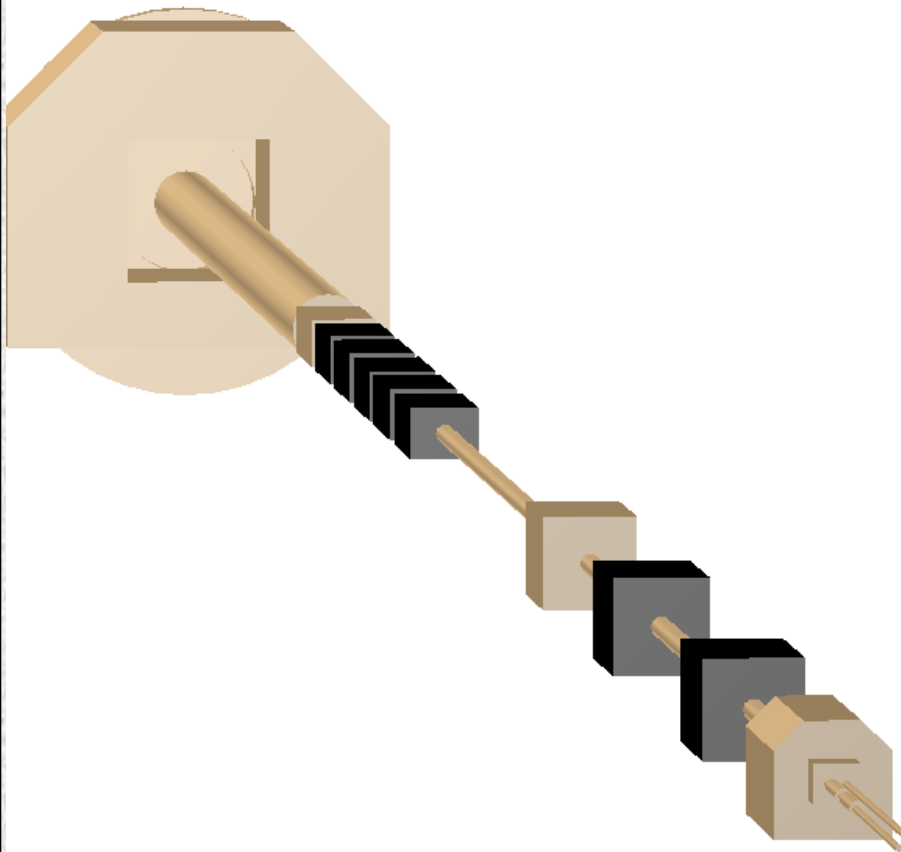
```
box-1      1 0 2  0. -5.  5. 10. 10. 15. 1 4 3
cyl-1a    -2 1 7  0.  0.  0.  0.  5. 20.
cyl-1a    -2 1 1  0.  0.  0.  5. 10. 20. 4 2
ball-a     3 0 8  0. 25. 20.  0.  5.
ball-b     3 0 3  0. 25. 20.  5. 10. 3
cone-in   -4 0 0  0. -30. 30.  0.  3.  0.  6. 20.
cone-out  -4 0 4  0. -30. 30.  3.  5.  6. 12. 20. 2 2
th        5 0 6  0. 0. 35. 5. 3. 55. 0. 20. 60. 0. -5. 65.
ell-tub1  -6 2 6  0.  0.  0.  8.  3.  0.  40.
ell-tub2  -6 2 5  0.  0.  0.  8.  3.  3.  40.
TR1 0. -15. 75. -20.
TR2 0.  30. 70.  20. 90.
stop
```



J-PARC Labyrinth Tunnel from Switchyard

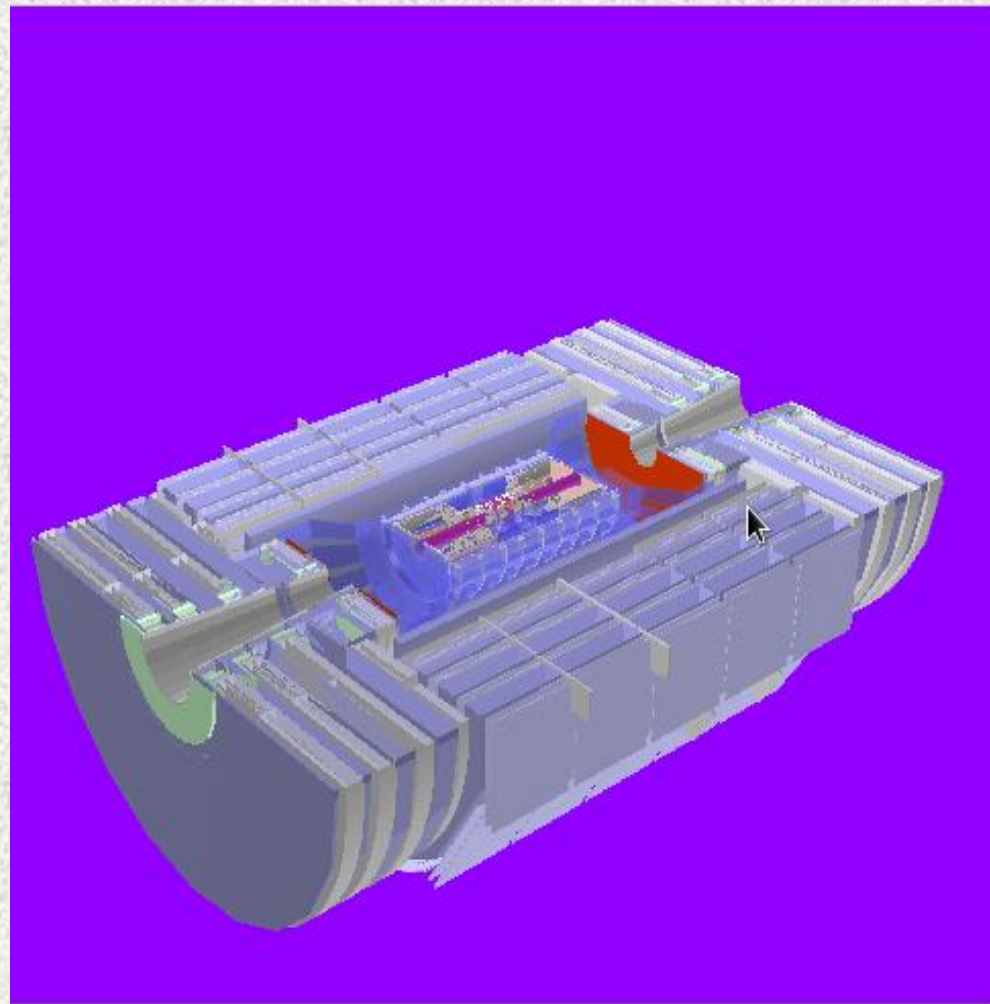


MARS15-ROOT: Built and Imported



ROOT geometry for the LHC IR5,
developed for MARS at FNAL

JAS, Newport Beach, CA, Nov. 7, 2014



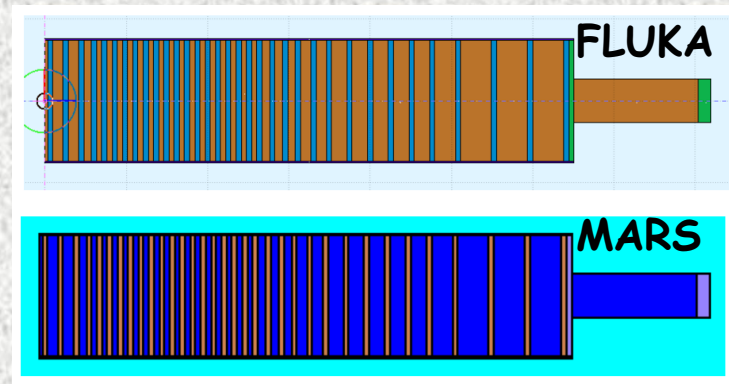
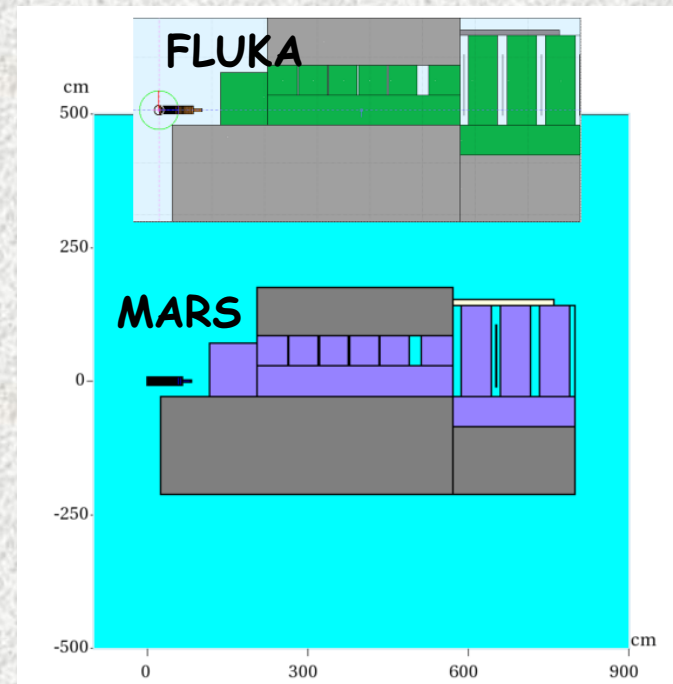
CMS ROOT geometry, developed in
CERN and imported to MARS15

Beam-Material Interactions, Part 1, Nikolai Mokhov

31

Geometry Converters

- **FLUKA-to-MCNP-to-MARS**
Available for about 10 years
- **FLUKA-to-MARS** by Sanami
Working prototype
- **MARS-to-FLUKA**
Possible if conjunction operation added
- **MARS: Extended-to-ROOT**
Working prototype
- **GEANT4-to-MARS-to-GEANT4**
Available using GDML format



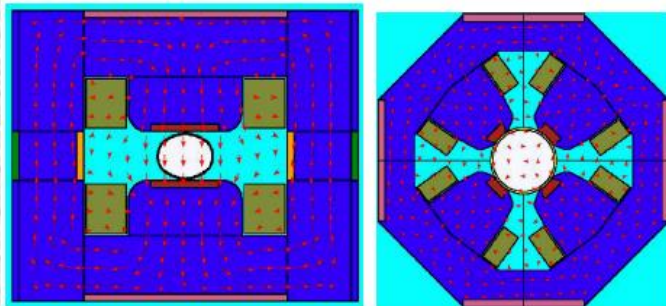
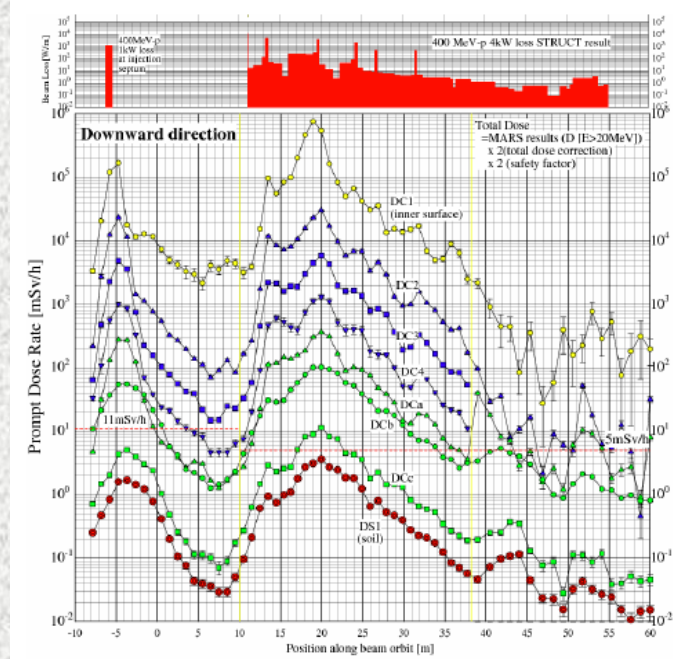
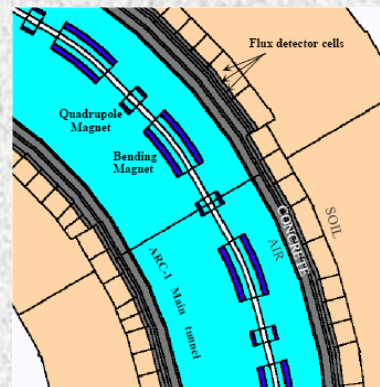
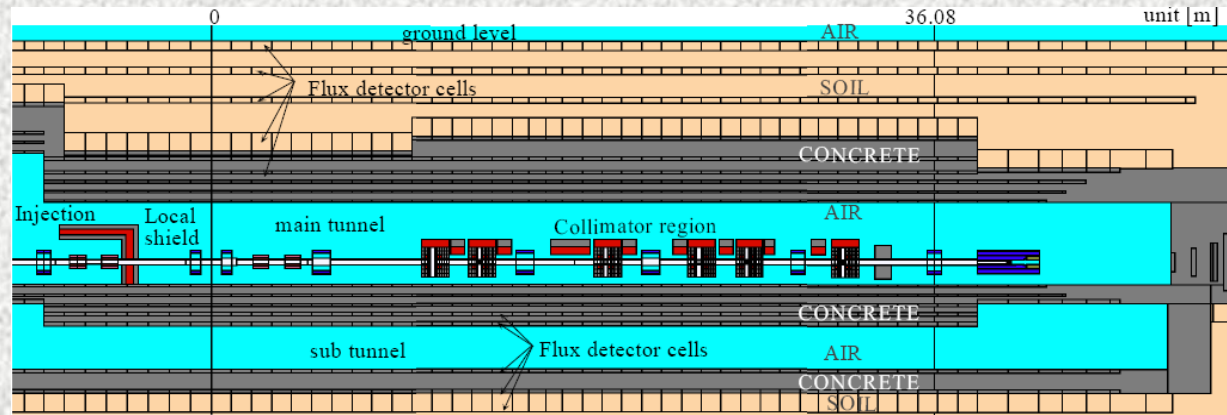
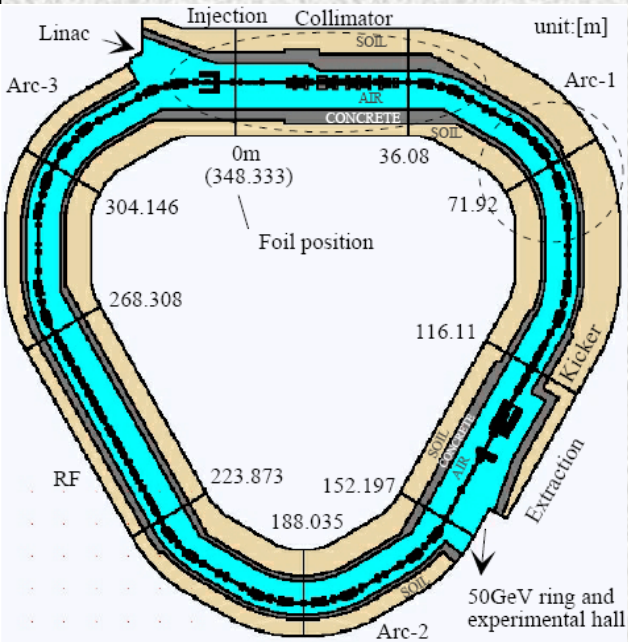
Automated Accelerator Geometry Generation and Accelerator-Shower Code Coupling

It is a modern approach for accelerator complexes to build a realistic model of the whole machine for beam loss, energy deposition, activation and radiation shielding studies:

Read in MAD lattice, create a complete 3-D geometry and magnetic field model, multi-turn beam transport throughout the lattice with lost particles transferred to FLUKA, Geant4 or MARS15 for full shower simulation.

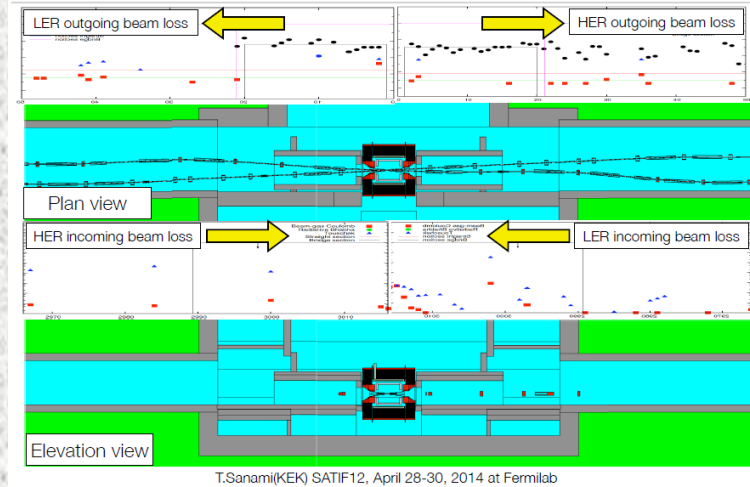
- MMBLB = MAD-MARS Beam Line Builder (since 2000); accelerator tracking using STRUCT with MARS modules. These days MARBL = MAD+MARS+ROOT
- BDSIM = accelerator-style particle tracking + full Geant4 power (since mid-2000s)
- SixTrack-FLUKA powerful active coupling (since 2013)

MAD-MARS BEAM LINE BUILDER: J-PARC 3-GeV RING

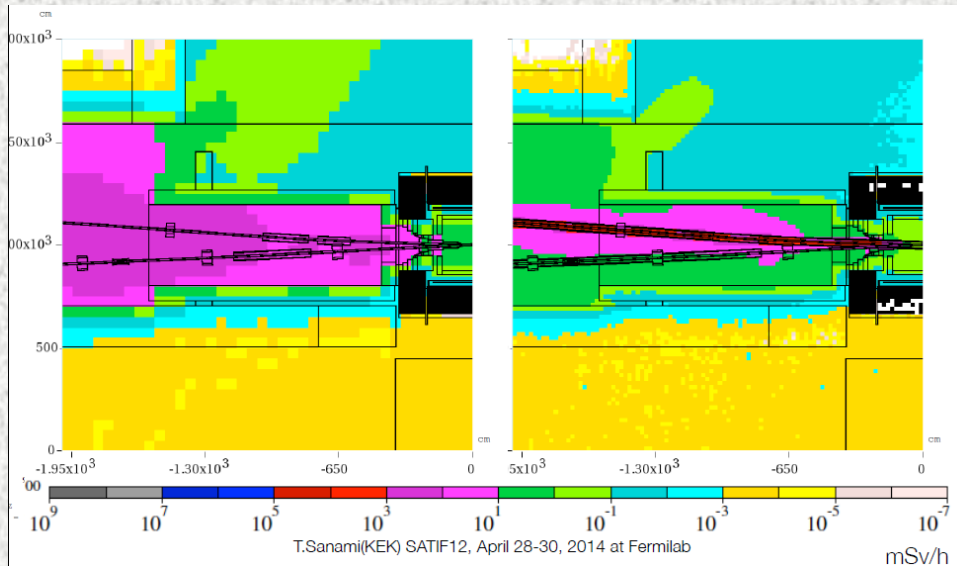
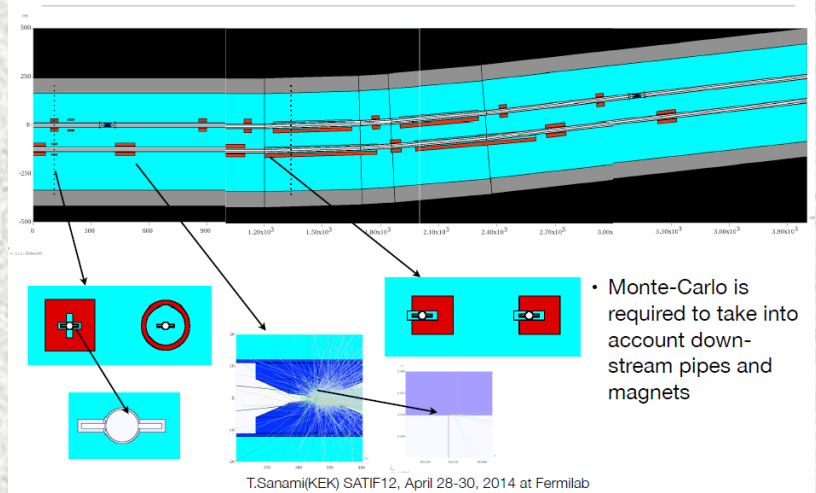


Super KEKB Factory MARS15 Studies

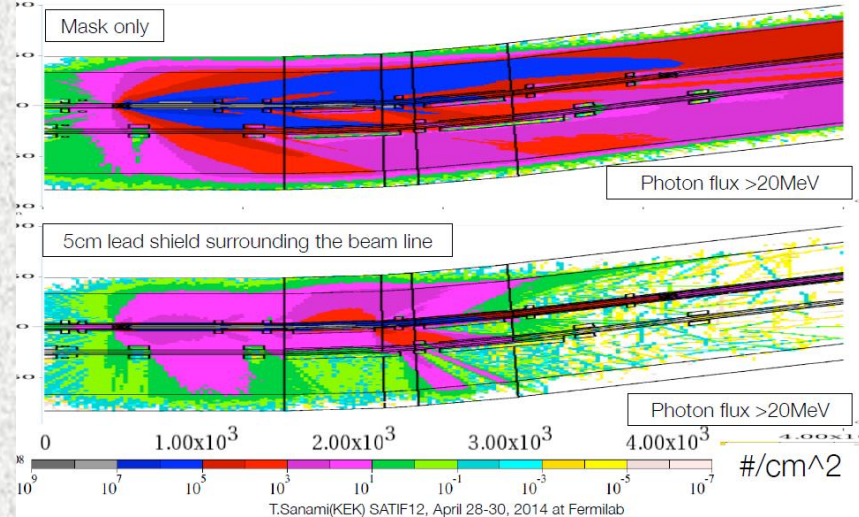
Detail geometry and beam loss modeling



Collimator and beam line modeling



Photon flux > 20 MeV

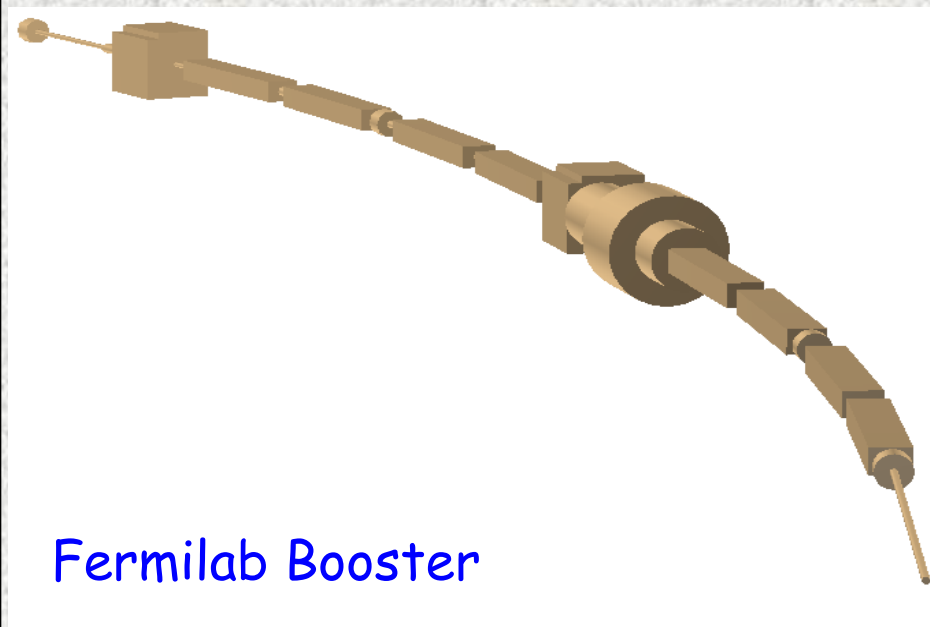


ROOT-Based MAD-MARS Beamline Builder

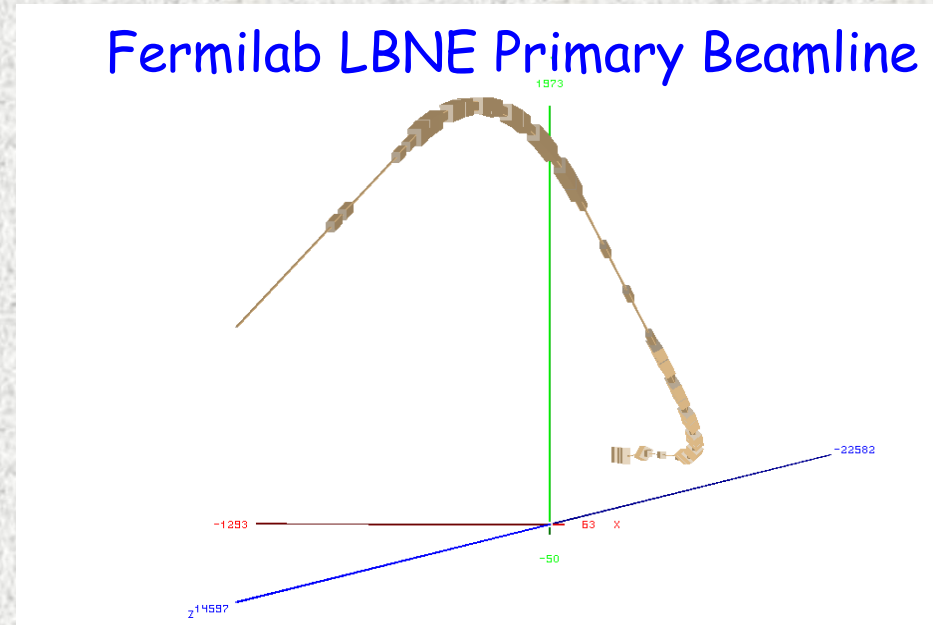
Set of functions (classes) for building beam lines, like MMBLB for non-standard MARS geometry.

Advantages as compared to MMBLB:

1. Unified highly precise approach
2. Eliminates possible misses of small objects at tracking time



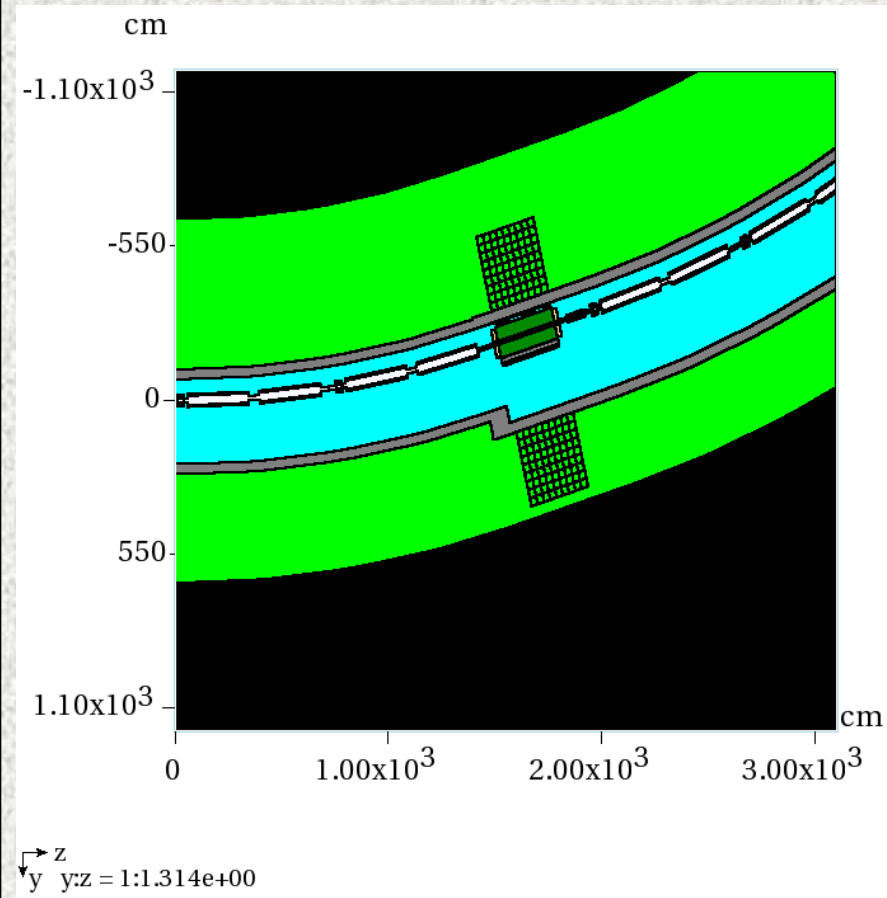
Fermilab Booster



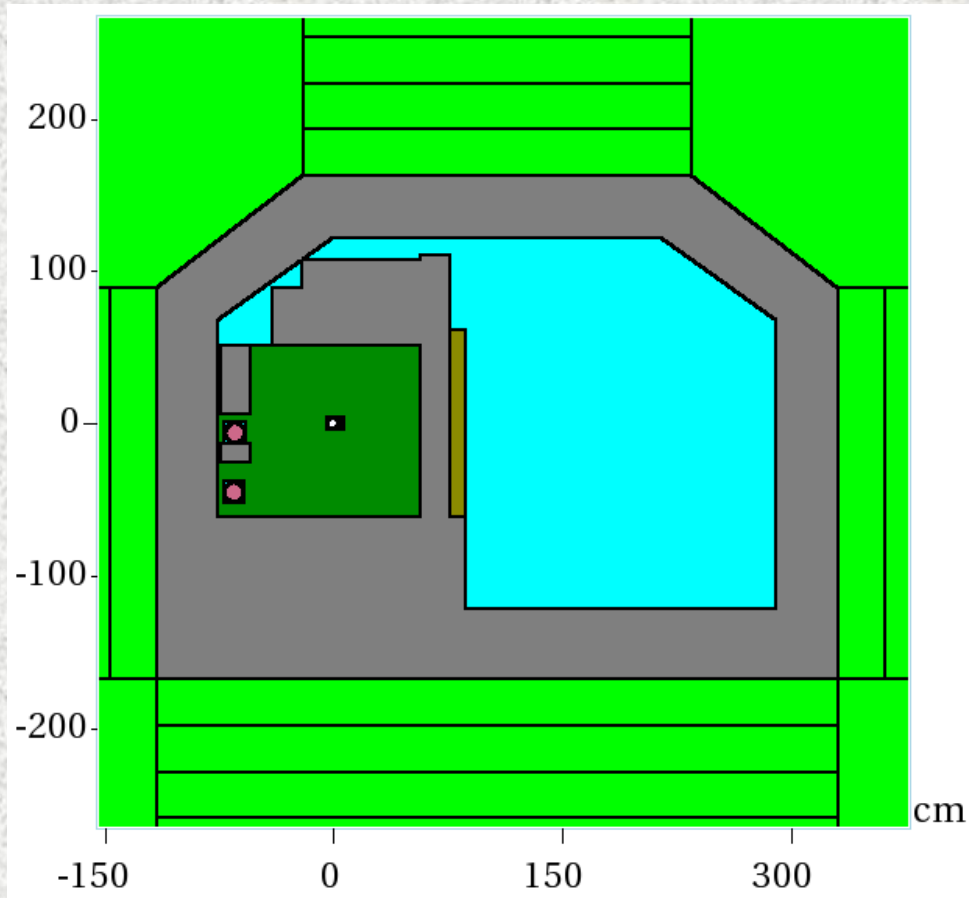
Fermilab LBNE Primary Beamline

MARS-ROOT Model of the Entire Fermilab Booster

8-GeV Booster



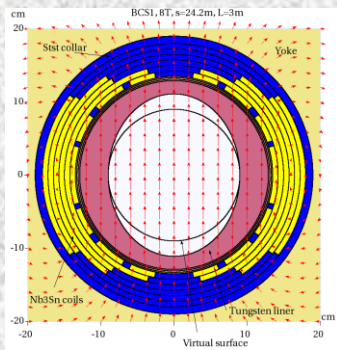
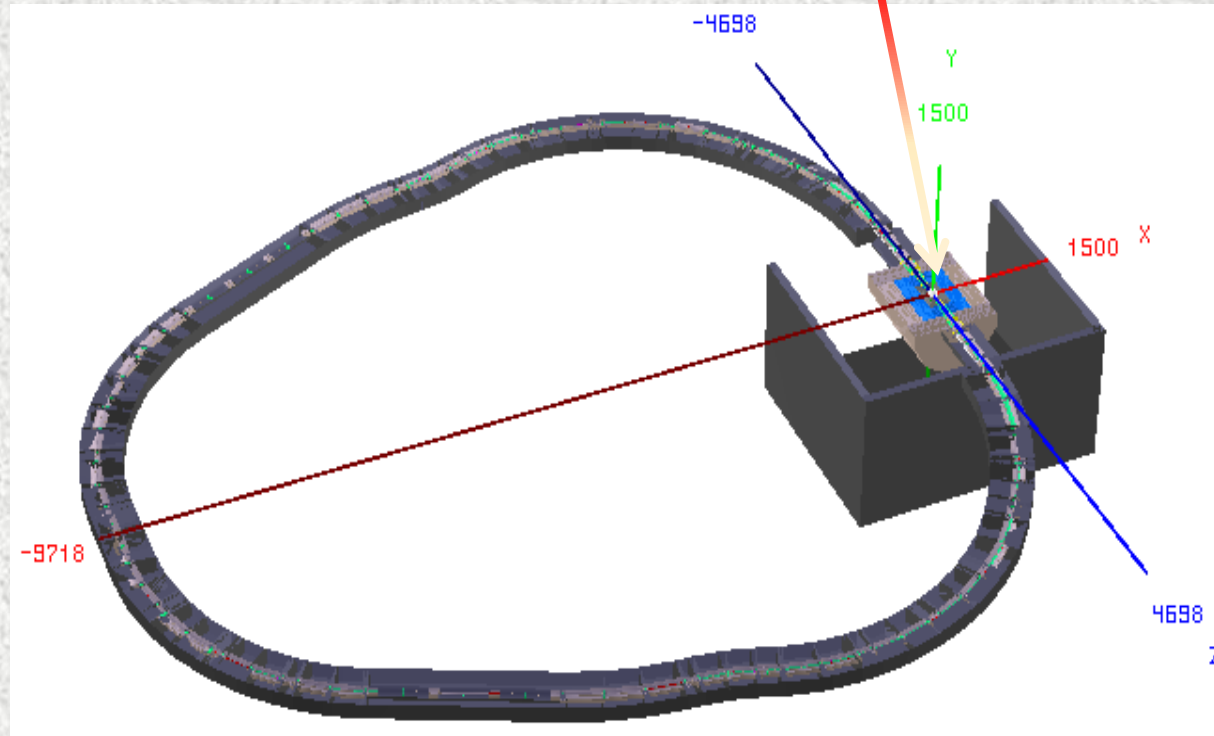
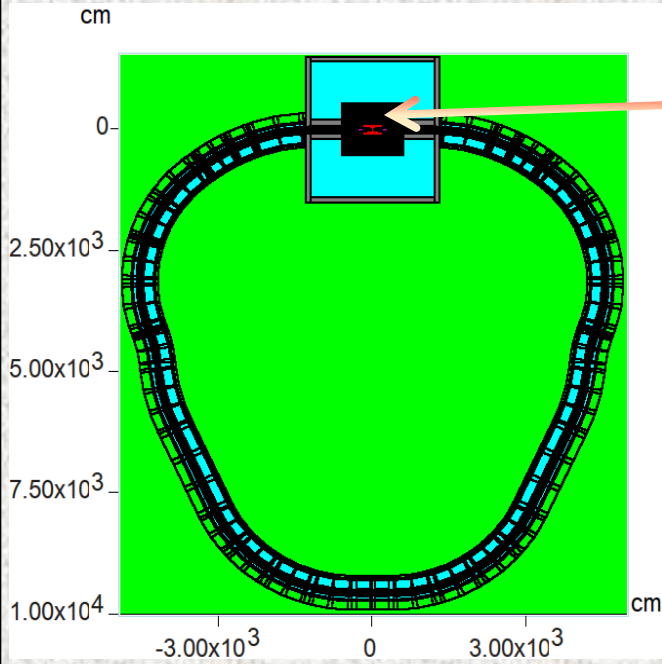
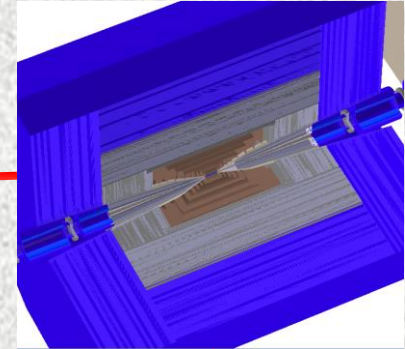
Collimator in tunnel



MARS-ROOT Model of Higgs Factory

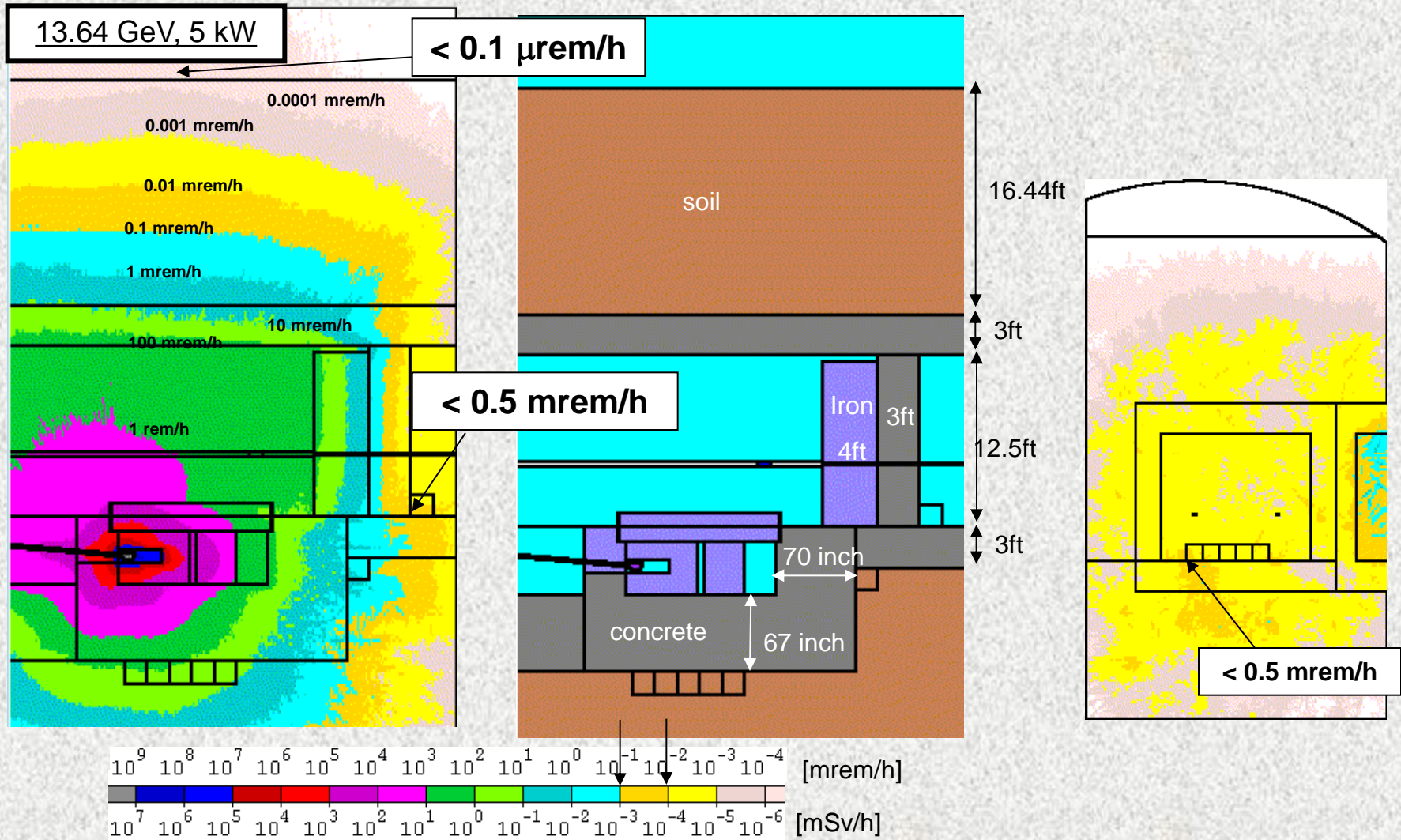
300-m $\mu^+\mu^-$ Collider

SiD-like detector with CMS upgrade-type tracker

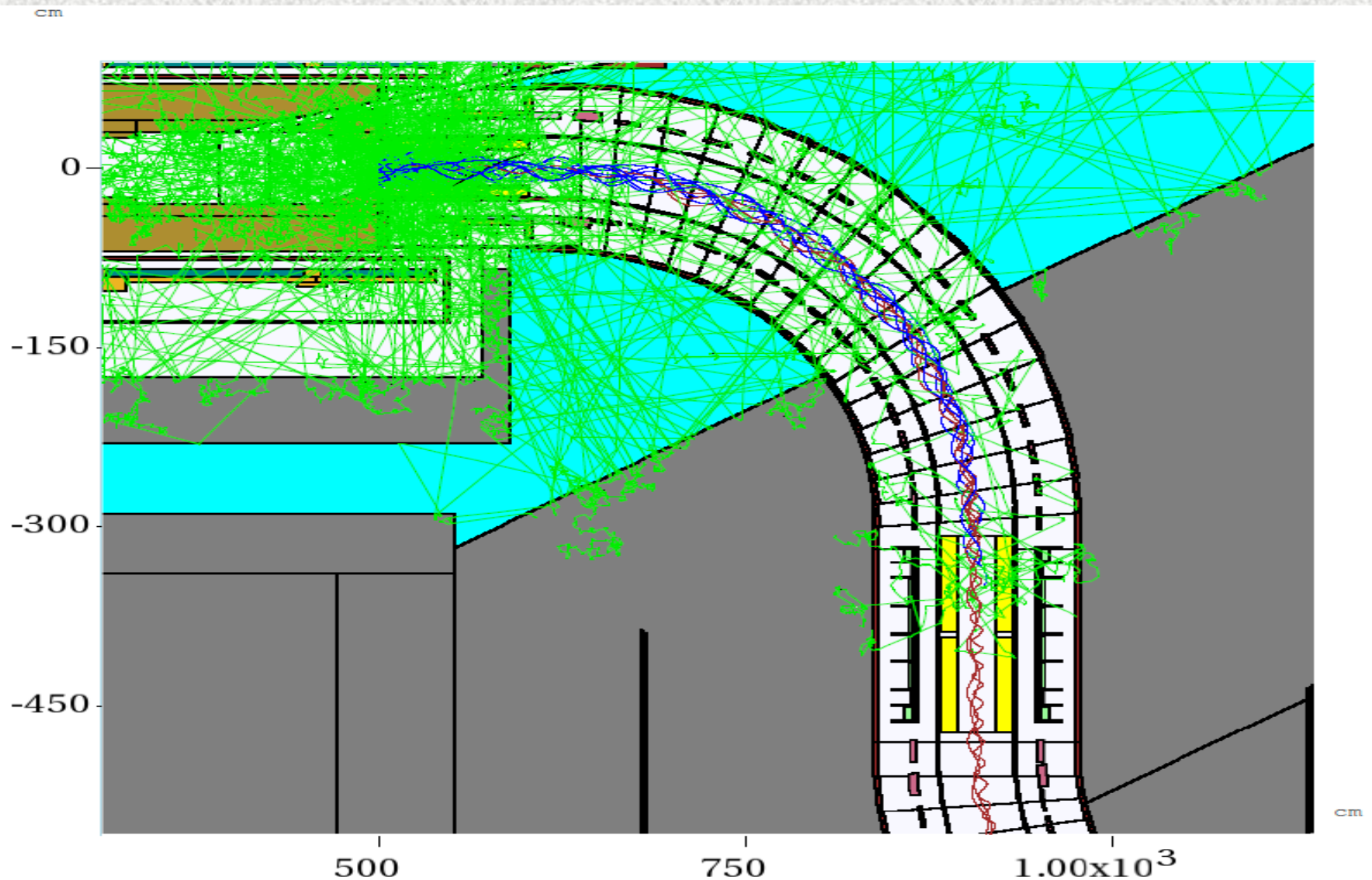


8-T
SC
dipole

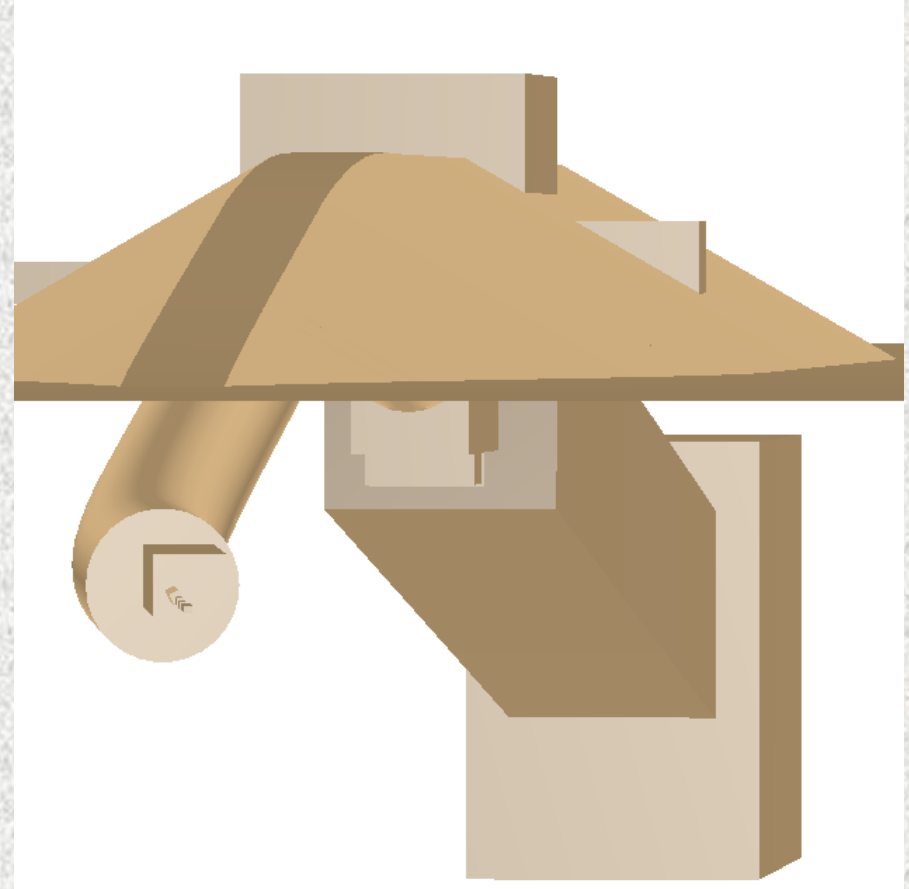
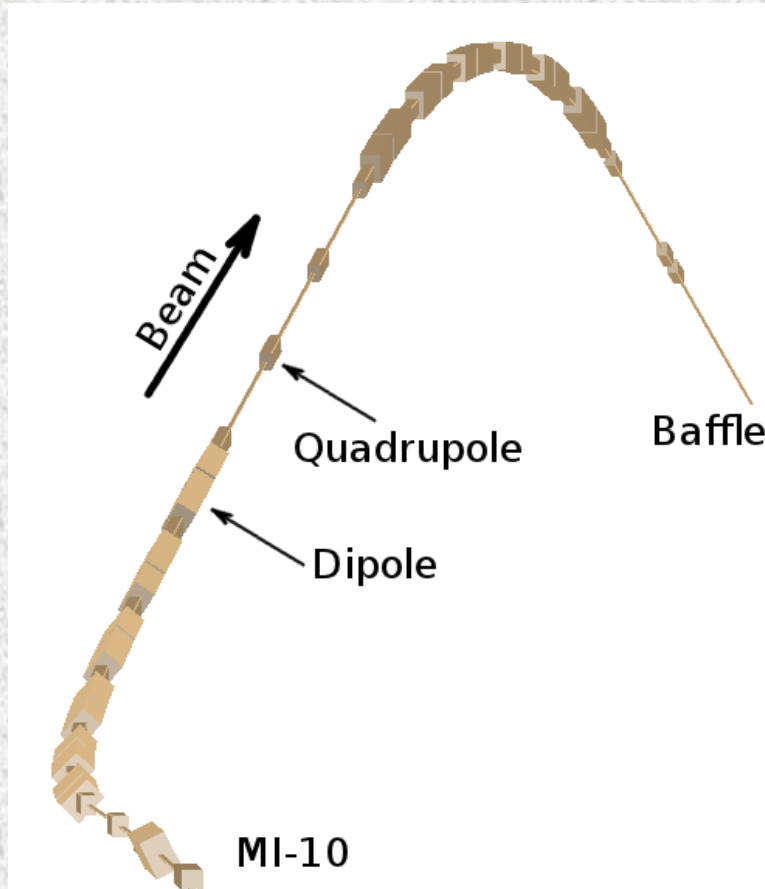
Example: MARS Dose Rate at LCLS



Mu2e: From Production to Transport Solenoid

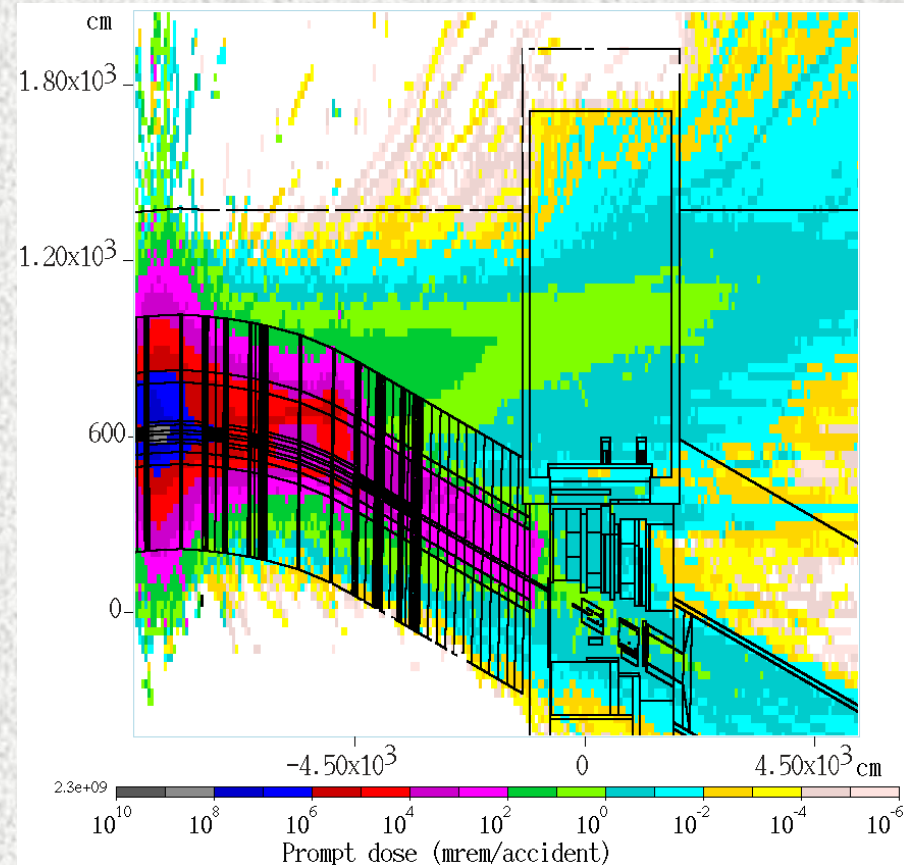
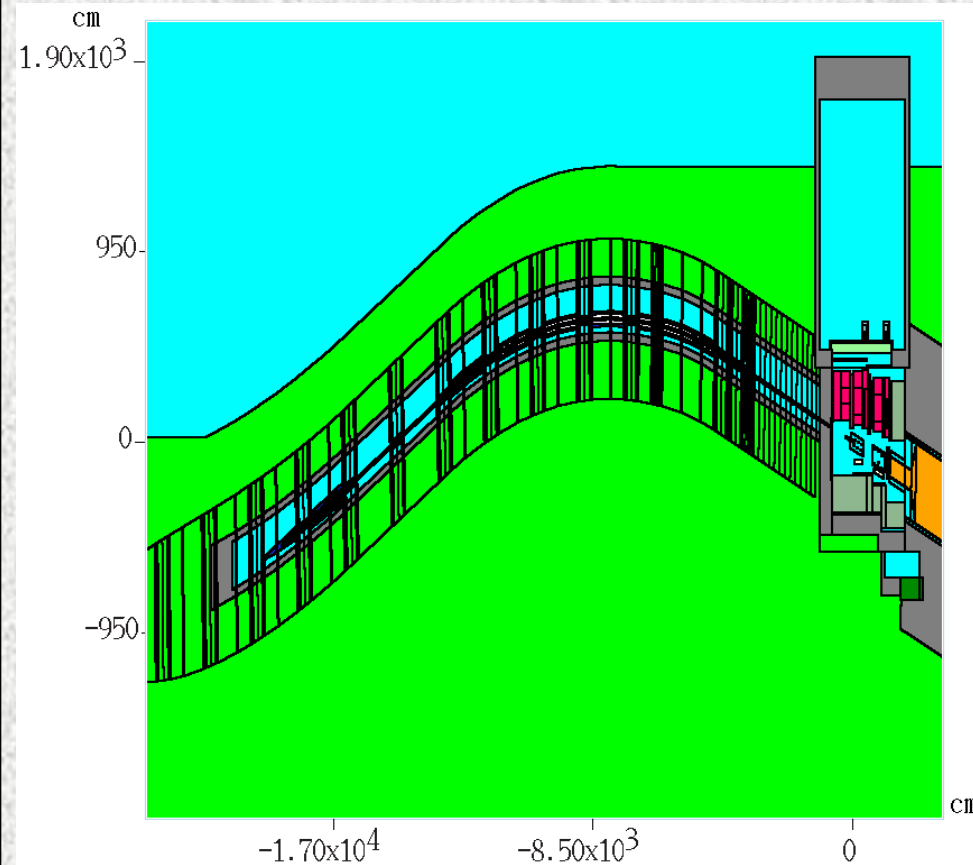


LBNE Primary Beamline MARS ROOT Model



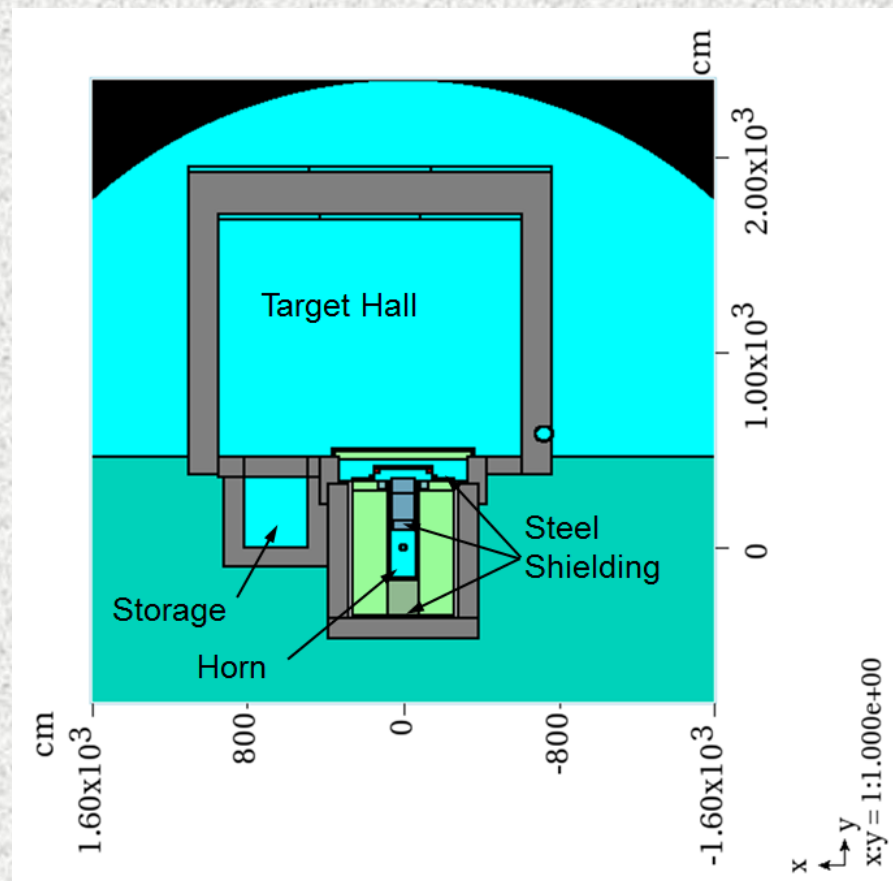
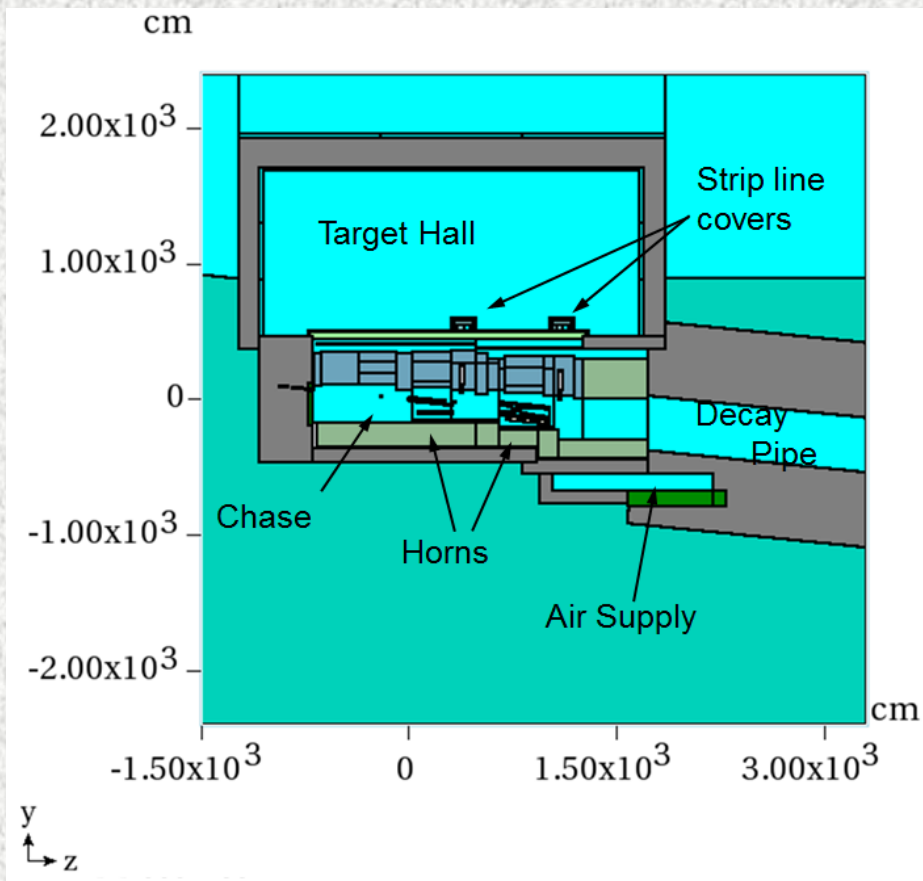
Studying operational and accidental beam loss distributions, impact on beamline components and environment, prompt and residual doses

LBNE: Muon Plum and Shielding at 3×10^{14} p/accident

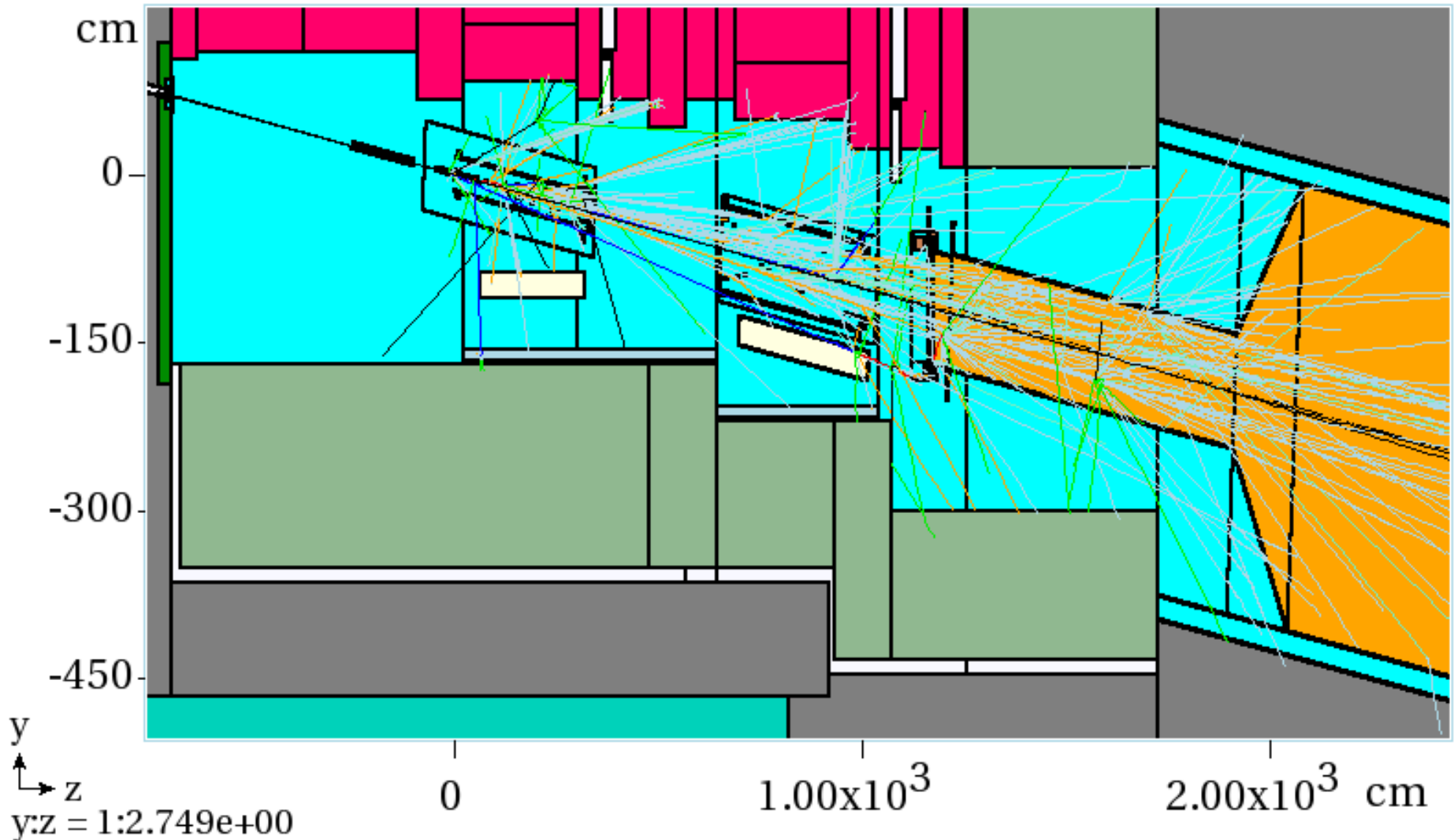


Worst-case accident in primary beamline: two sequent 120-GeV full beam pulses lost locally at the apex \rightarrow beampipe destruction and μ -shielding driven

LBNE Target Chase

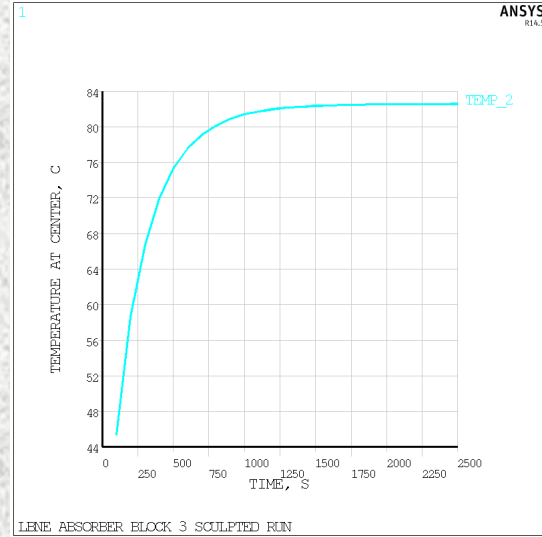
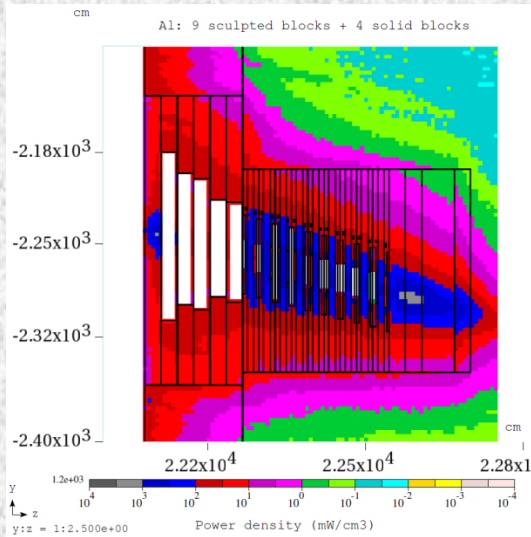


Tracks for He in Snout & DK

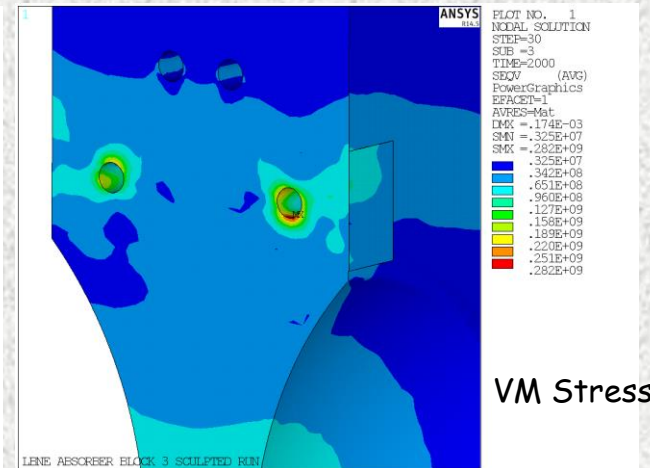
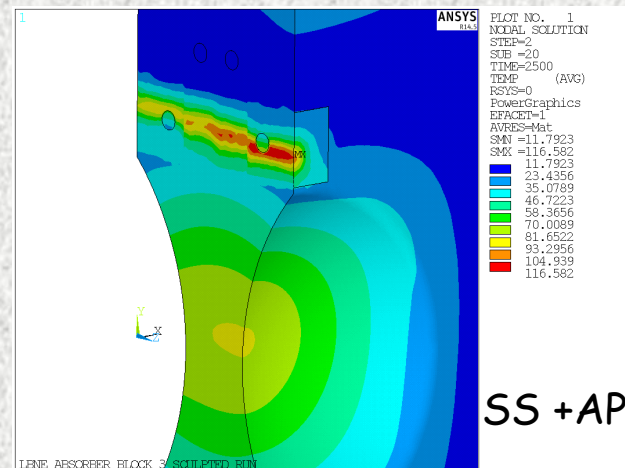
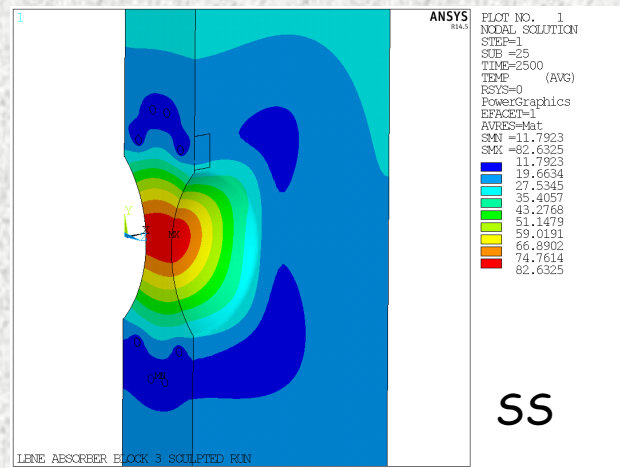


Energy Deposition, Temperature and Stresses

Detailed energy deposition maps with MARS15 in core hot regions for normal and accidental cases to feed ANSYS

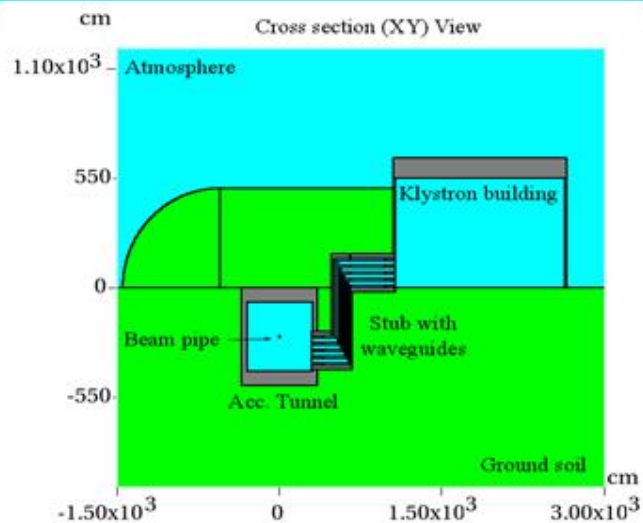


ANSYS runs for normal case to reach steady state followed by on-axis or off-axis accident pulse

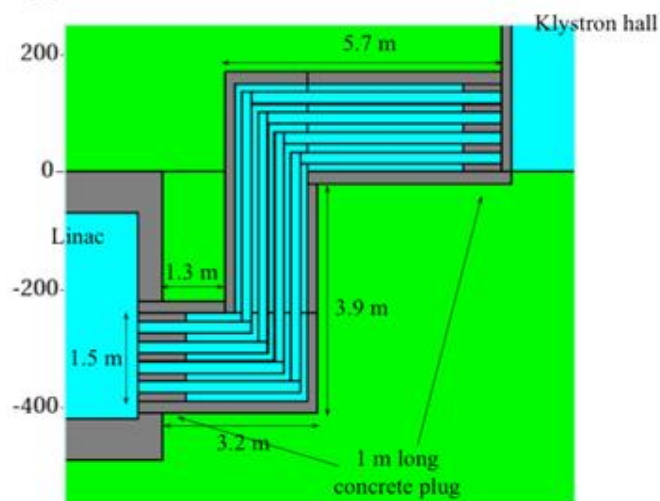


See more in Bertarelli's lecture tomorrow

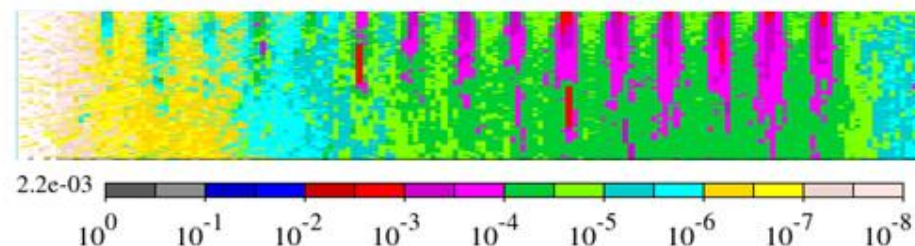
RF waveguide penetrations Stubs



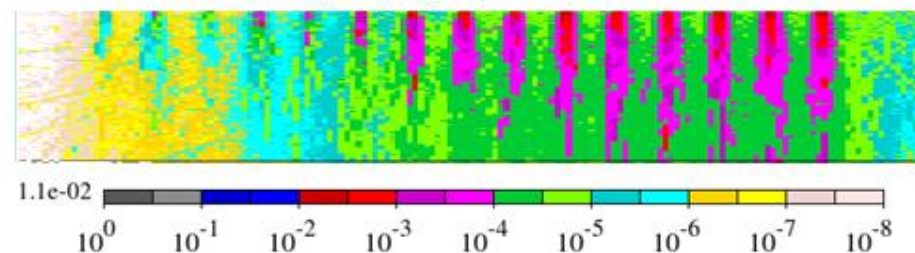
x
y
xy = 1:2.045e+00



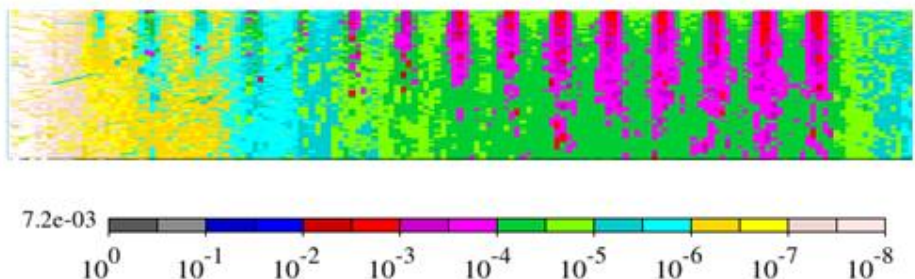
DET (mSv/h) Top view at ground level



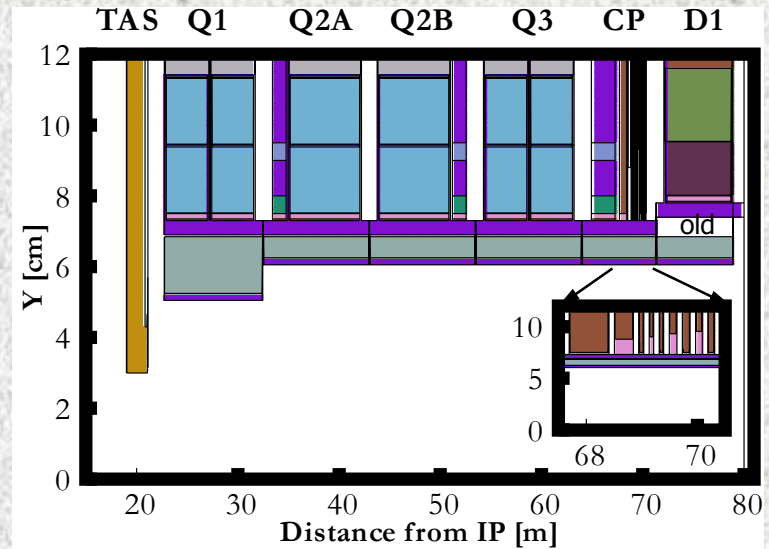
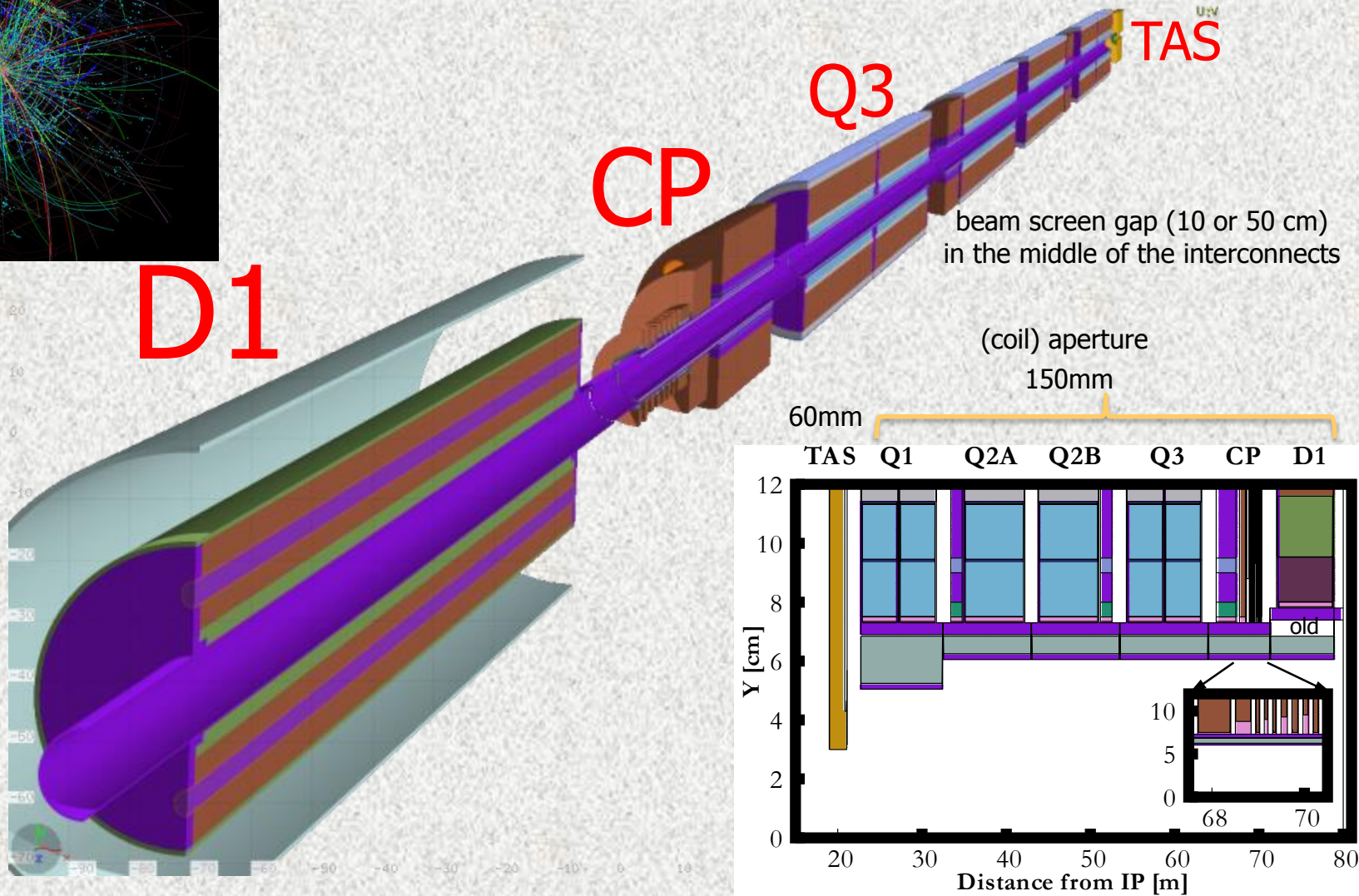
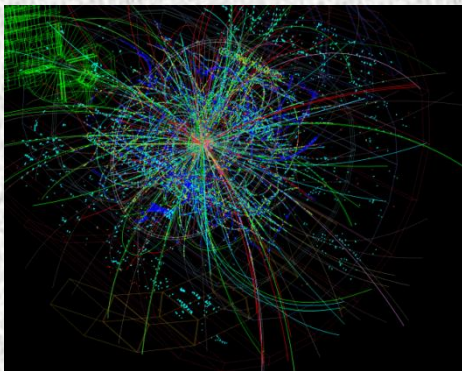
DET (mSv/h) Top view at 1 m



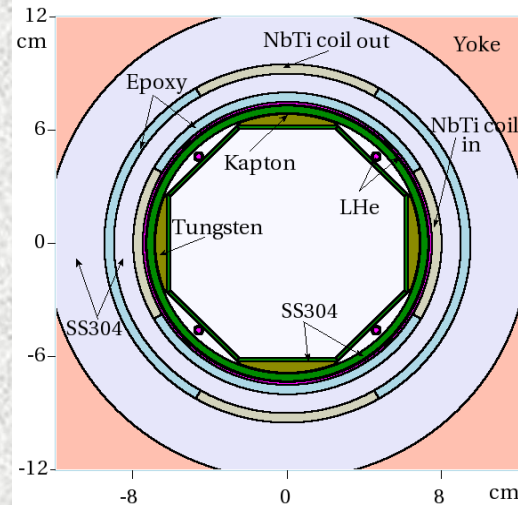
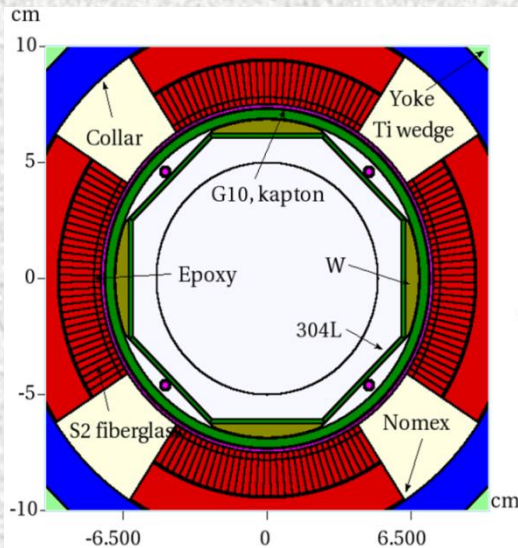
DET (mSv/h) Top view at 2 m



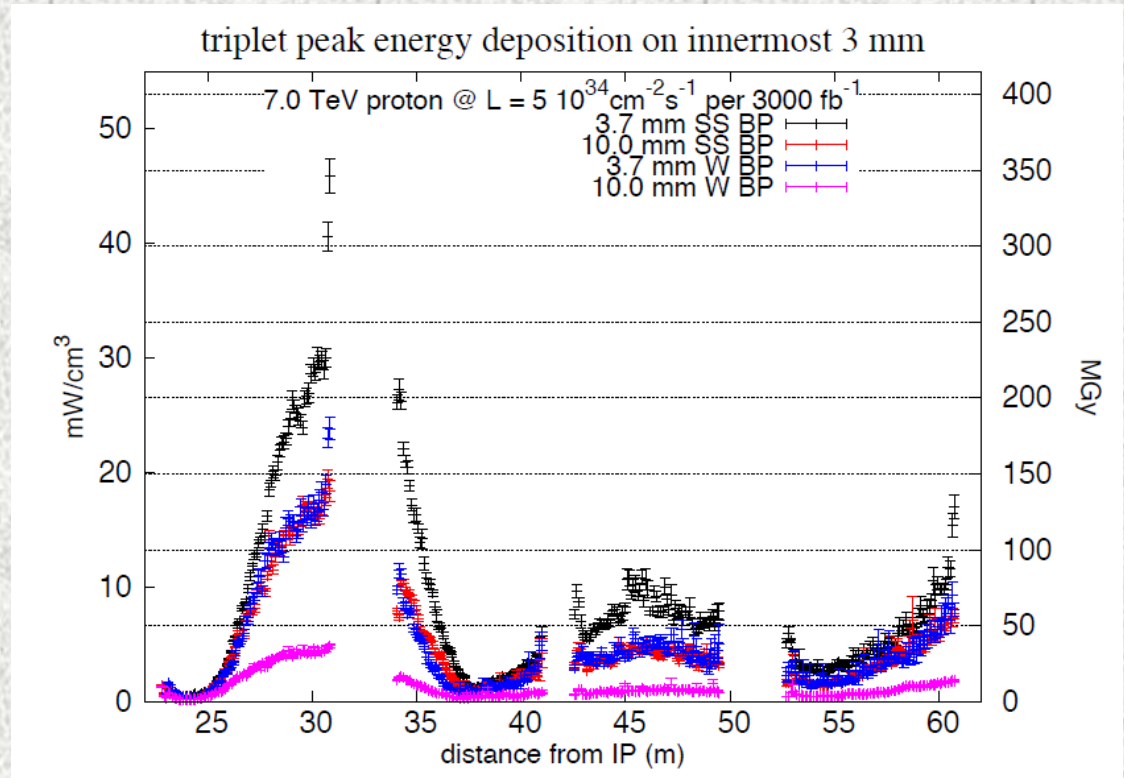
Hi-Lumi LHC Inner Triplet



Tungsten Absorbers in IT Aperture

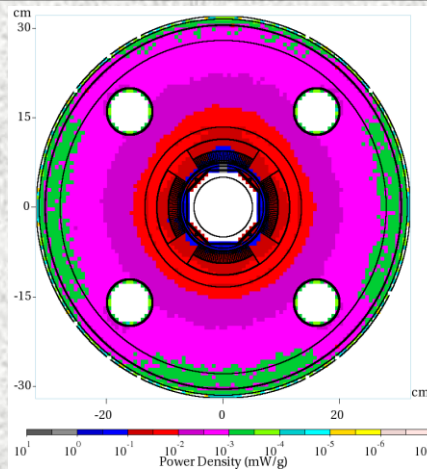
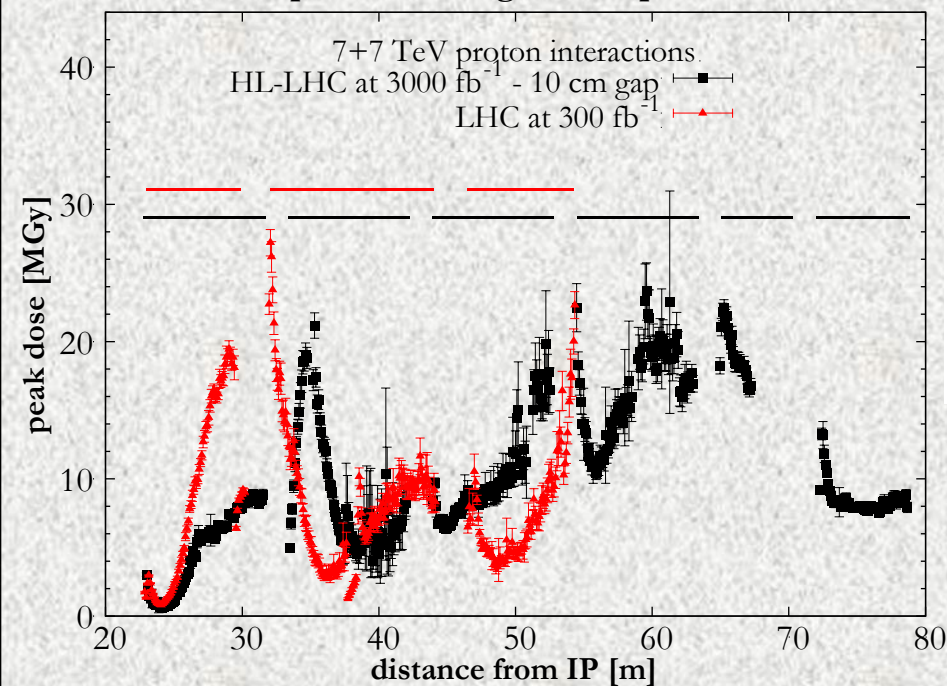


Early studies of inner tungsten absorber effectiveness



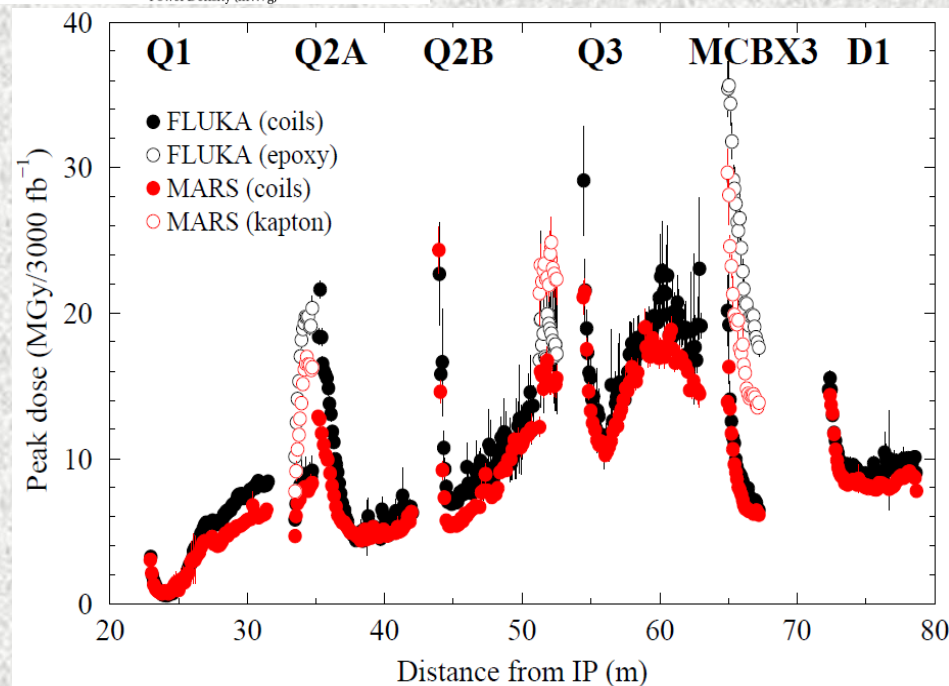
Hi-Lumi LHC Upgrade: "Beam Loss and Accelerator Protection"

peak dose longitudinal profile

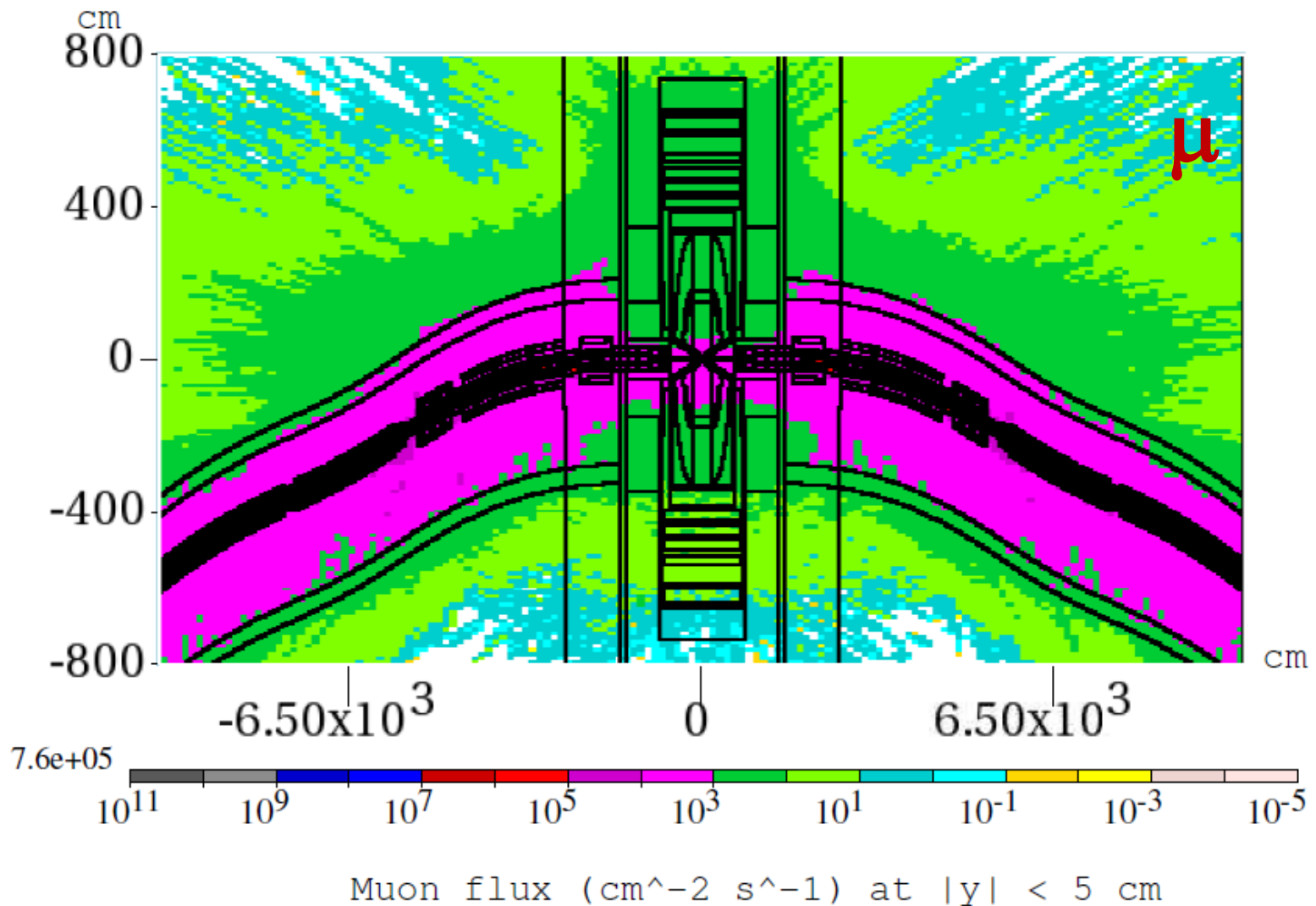


FLUKA & MARS
correlated studies:
design goals achieved

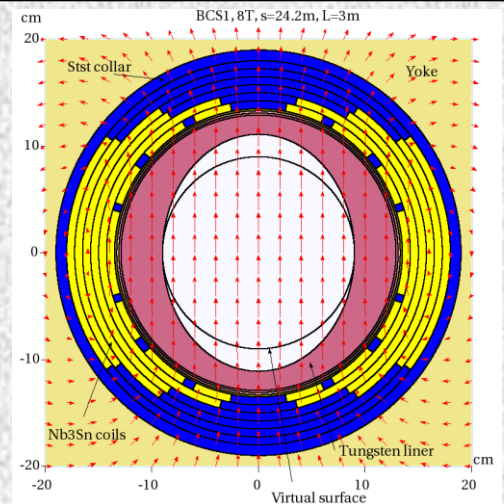
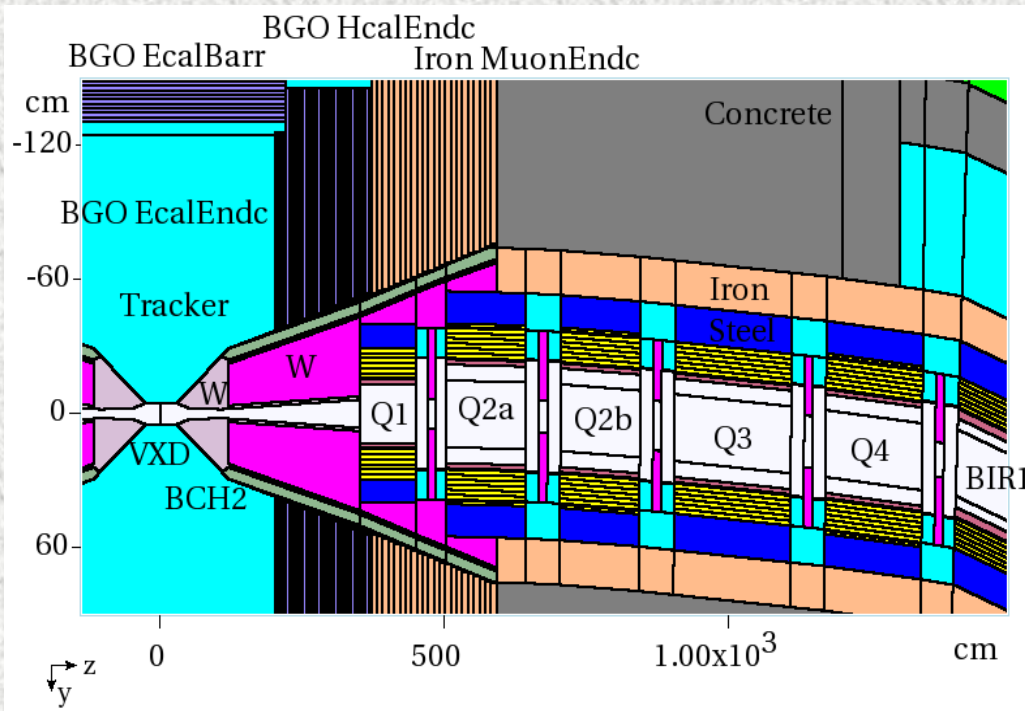
With proposed protection system,
peak dose (i.e. lifetime) in HL-LHC
magnets at 3000 fb⁻¹ is the same as
in LHC magnets at 300 fb⁻¹ !



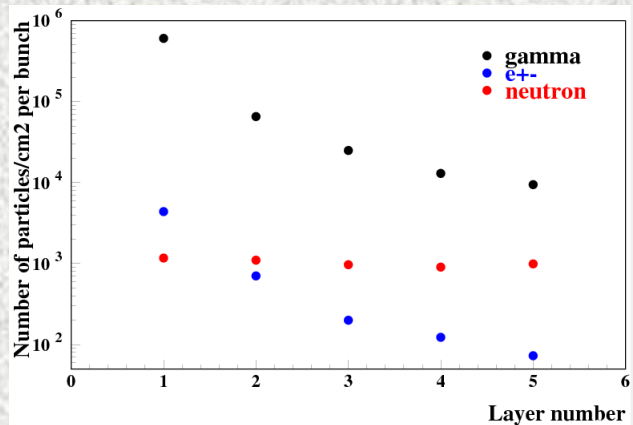
1.5-TeV Muon Collider



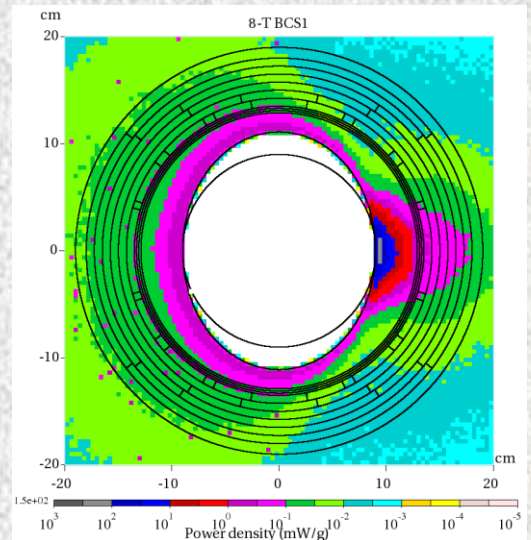
Higgs Factory Muon Collider (HFMC)



Tungsten inner absorber and power density

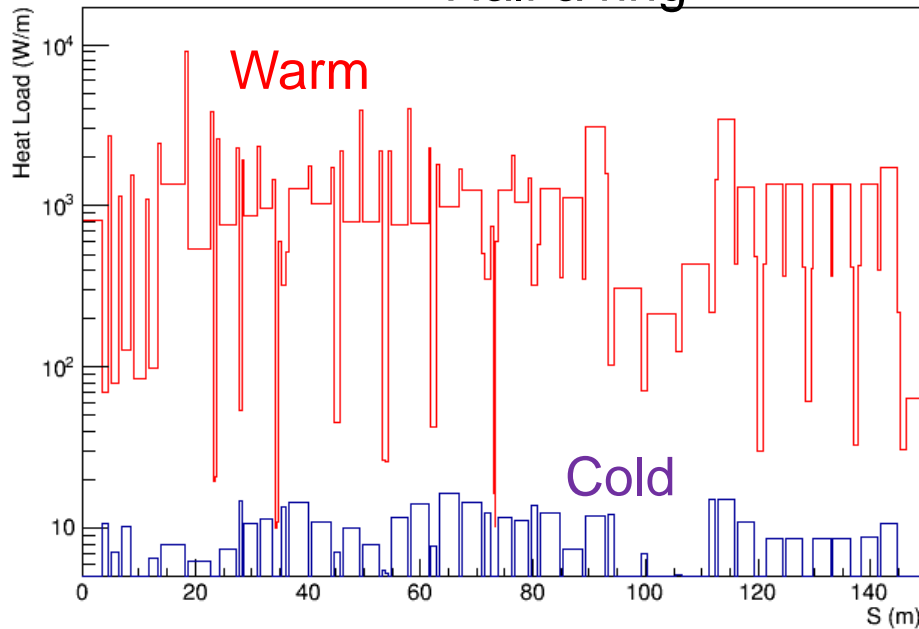


Fluxes of background particles in VXD with appropriately designed Machine-Detector Interface (MDI) to protect IR magnets and detector components.

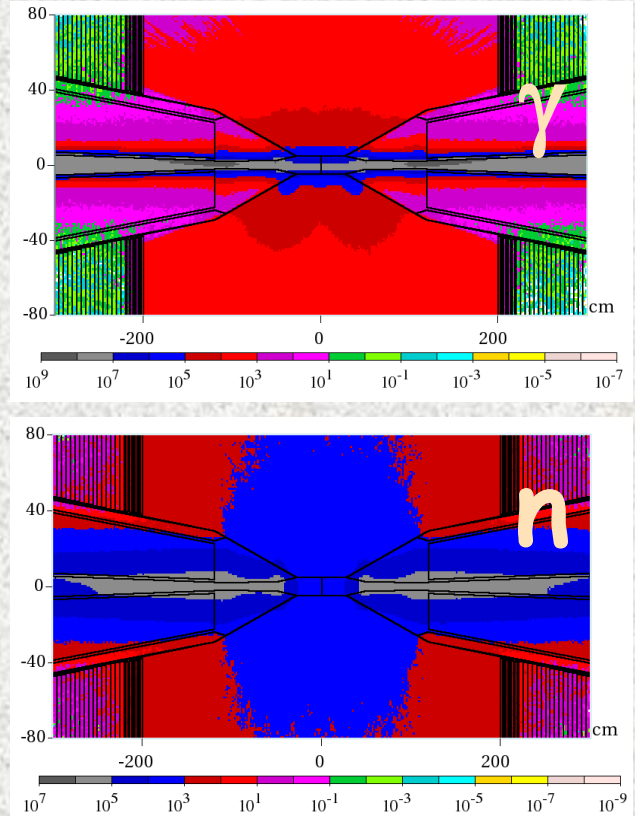


HFMC: "Beam Loss and Accelerator Protection"

Half a ring



With thick tungsten masks in interconnect regions and inside superconducting magnets, able to reduce average dynamic heat load of ~1 kW/m to the allowable 10 W/m at 4.5K and keep the peak power density in the coils below the quench limit with a necessary safety margin.



Based on thorough Monte-Carlo, carefully designed massive W-inserts and MDI along with sophisticated tight W-nozzles near IP: ~1000 reduction of heat loads on IR magnets and background loads on detector.

Many thanks to

F. Cerutti, L. Esposito, K. Gudima, P. Hurh,
S. Mashnik, N. Nakao, V. Pronskikh, I. Rakhno,
T. Sanami, S. Striganov, T. Suzuki, L. Tchelidze,
and I. Tropin for fruitful collaboration over many
years and some figures used in this lecture.